Index

North Sea FLOW Measurement Workshop

Paper 3.1

Ultrasonic Flare Gas Flow Meter Techniques for Extremes of High and Low Velocity Measurement and Experience with High CO2 Concentration

Jed Matson
GE Sensing & Inspection Technologies

Lei Sui
GE Sensing & Inspection Technologies

Toan H. Nguyen
GE Sensing & Inspection Technologies

TÜV SÜD

nel technology for life

Ultrasonic Flare Gas Flow Meter Techniques for Extremes of High and Low Velocity Measurement and Experience with High CO2 Concentration

Jed Matson, GE Sensing & Inspection Technologies
Lei Sui, GE Sensing & Inspection Technologies
Toan H. Nguyen, GE Sensing & Inspection Technologies

1 INTRODUCTION

The ultrasonic transit time gas flowmeter has been established as the preferred method for Flare Gas flow measurement with more than 3000 units installed worldwide in process plants and refineries, on and offshore. New requirements around total emissions have been, or are being, implemented around the world and this presents additional technical challenges for ultrasonic flowmeters in the areas of (1) extremely low flare flow rates (0.3 m/s and below) during normal, or base load flaring, (2) extremely high flare flows (80 m/s and above) during emergency flaring and (3) measuring the flow rate of gas with a high CO_2 concentration. Low flare flows are influenced and asymmetric due to convection flow and stratification; High flare flows introduce soaring flow noise, cause ultrasonic beam drift and thus deteriorate ultrasonic signal quality. High CO_2 gas concentration can drastically attenuate ultrasonic energy.
In this paper, the uncertainty of flow rate at low flow is examined and demonstrated in the typical large diameter flare gas pipes. Techniques for improving the uncertainty of flow at low velocity, both for required resolution, and for better area averaging of asymmetric flow profile are presented. The ultrasonic signal propagation in (flare) gas has been studied, the beam drift due to gas flow has been investigated and improvements from both mechanical and transducer perspectives have been made to compensate for these two problems. An improved version of the flare gas ultrasonic meter has been developed to demonstrate the accurate measurement of air flow up to 123.7 m/s. Testing data have been presented for two typical configurations, Bias 90 and Diagonal 45, in comparison with a Venturi reference meter. The overall accuracy of the new flare meter is demonstrated to be 3-4%, and the relative standard deviation of the meter readings is within 1.2%. In addition specific applications of the flare gas flowmeter to gases with high CO_2 concentration, as high as 100%, are examined and the solutions are described

2 HIGH VELOCITY FLOW

Flare systems are primarily installed for safety purposes in chemical, petrochemical, refining, and other plants. These flare systems are used to vent and burn off hydrocarbons and other unwanted gases under routine and emergency conditions, such as an unexpected shutdown. Today there is an international awareness to measure and monitor flare gas flow for both environmental and economical reasons [1][2][3]. The measurement of flare gas helps to comply with environmental regulations, identify points of leakage, and reconcile plant mass balance.
Flare gas flow measurement itself is challenging mainly due to factors such as: unsteady flow velocity, pressure fluctuations, variable composition, aggressive chemicals in the gas, potential high temperature excursions and a wide-range of flow rates. In particular, it requires instrumentation to be capable of measuring gas flow over a wide range of velocities: from 0.03 m/s low flow, through 0.15-0.5 m/s for most normal operations, and up to 80 m/s and above during emergency flaring.
In the early 1980s, a flare gas ultrasonic flowmeter was first jointly developed by Panametrics (now GE Sensing) and Exxon (now ExxonMobil) in Baytown, Texas, USA. [1]. Since then, ultrasonic flowmeters have been gaining more and more popularity for flare gas measurement, mainly because of its high turndown ratio, its relatively low installation and maintenance costs, its capability of handling unsteady flows, and its independence from gas composition. Today, the ultrasonic flow meter is the accepted technology for monitoring flare gas, with more than 3,000 installations worldwide.
Although flare gas ultrasonic flowmeters have evolved with many improvements over the past 25 years, one of the remaining technical challenges is to deal with extremely high flow velocity up to 80 m/s and above. Such high flare gas flows can occur during a process shutdown when all the process gases need to be flared. A poor signal quality at high flow velocities, usually quantified by low signal-to- noise ratio (SNR), is due to such factors as beam drift, greatly-increased noise level, and

turbulence-related attenuation, that cause scattering and distortion of ultrasonic signals [4]. As a result, flare gas ultrasonic flowmeters available on the market today offer the maximum velocity typically of 85 m/s – 100 m/s [5][6].
An ultrasonic flowmeter has been developed and tested for high-velocity gas measurement up to 123.7 m/s in air. The enabling technologies behind this new development are design of the transducer dimensions, transducer separation and operating frequency, and the implementation of a recovery angle to the downstream transducer. Testing results obtained from a wind tunnel in the Energy and Propulsion Technologies Laboratory at the GE Global Research Center located in Niskayuna, NY is presented. The accuracy of the new meter is demonstrated to be better than 3-4% with reference meter uncertainty included, and the relative standard deviation of the new meter is within 1.2%.

2.1 Methodology: Design of Transducer Dimensions, Separation, and Frequency

Using ultrasound to measure flow velocity has been a well-known technique for decades [7]. Transit-time ultrasonic flowmeters take advantage of a simple principle, called “time of flight”, as illustrated in Fig. 1. Specifically, the time it takes for an ultrasonic signal to travel against the flow (i.e., upstream), t_{up}, is longer than the time it takes with the flow (i.e., downstream), t_{dn}. The difference between upstream and downstream transit times, Δt, is directly proportional to the flow velocity as follows [8][9]:

$$V = \frac{P}{2\cos\theta}\left(\frac{1}{t_{dn}} - \frac{1}{t_{up}}\right) = \frac{P}{2\cos\theta}\left(\frac{\Delta t}{t_{dn}\ t_{up}}\right), \qquad (1)$$

Where V is the flow velocity to be measured, P is the ultrasonic path length, and θ is the acute angle between the ultrasonic path and the axis of the flowcell or pipe section.

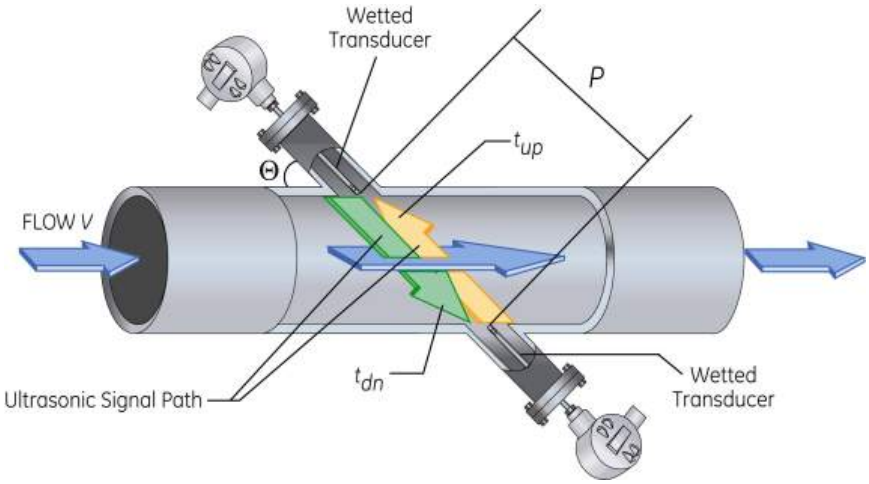

Figure 1. The operating principle of a transit-time based ultrasonic flowmeter.

From Eq. (1), it can be seen that the measurement strongly depends on the timing of t_{up}, t_{dn}, and Δt. The measurements of t_{up}, t_{dn}, and Δt rely on the quality of the received ultrasonic signal, i.e., signal-to-noise ratio (SNR).
For linear ultrasound propagation, there exist near-field and far-field regions, with the latter beginning at the so-called Rayleigh distance [10].

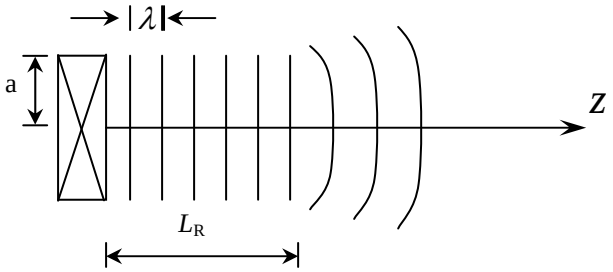

Figure 2. Ultrasound propagation in a medium across both near field and far field nominally separated by Rayleigh Distance, L_R.

In the far field, the pressure amplitude at location z (which is measured along the transducer axis with $z = 0$ starting at the transducer surface), *P* (*z*), can be approximately written as [11]:

$$P(z) = K_0 \frac{a^2}{z} e^{-\alpha z}, \qquad (2)$$

Where K_0 is a constant determined by the driving amplitude of the transducer, efficiency of the transducer, and the medium in which ultrasound is propagating, and α is the ultrasonic attenuation coefficient in units of neper/m or dB/m. The ultrasonic attenuation coefficient depends on the medium in question and is typically a function of the ultrasonic frequency by the power law as:

$$\alpha = \alpha_0 f^n, \qquad (3)$$

In which α_0 and *n* are two coefficients used to describe this function. In practice, both α_0 and *n* could be obtained by measuring ultrasound pressure at different frequencies and distances.

Substituting Eq. (3) into Eq. (2), we obtain:

$$P(z) = K_0 \frac{a^2}{z} e^{-\alpha_0 f^n z}. \qquad (4)$$

Eq. (4) indicates that to increase the ultrasonic signal amplitude, it is desirable to have transducers with a large radius (or diameter), to keep the separation of the transducer pair close, and to select a relatively low ultrasonic frequency. In reality, the transducer dimensions are limited by the cost of the transducers, the mechanical arrangement associated with the transducers, and the openings in the flowcell; the larger openings on the pipe tend to disturb the local flow profile. Similarly, the separation of the transducers is restricted by the accuracy requirement at low flow rates. Finally, the selection of an ultrasonic frequency is a trade-off between maximizing resolution and minimizing attenuation. Taking the above compromises into consideration, the transducer design has a radius of 0.375" and a frequency of 100 kHz (refer to [13] for more transducer details), and a separation of the transducer pair of ~6.5 to 7.8".

2.2 Recovery Angle

One difficulty with ultrasonic measurement of high velocity flare is ultrasonic beam drift. The high velocity will blow the ultrasonic signal away and this will result in a miss of the "perfectly aligned" targeted receiving transducer. We can calculate the downstream beam drift angle γ due to flow velocity *V* in a gas medium characterized by its speed of sound *c* as follows:

$$\gamma = \theta - \arctan\left(\frac{c\sin\theta}{c\cos\theta + V}\right) = \theta - \arctan\left(\frac{\sin\theta}{\cos\theta + M}\right), \qquad (5)$$

Where θ is as defined above, i.e., the acute angle between the ultrasonic propagation and flow directions, and $M = V/c$ is the Mach number. Similarly, the upstream beam drift angle γ can be derived as follows:

$$\gamma = \begin{cases} \theta - \arctan\left(\dfrac{\sin\theta}{\cos\theta - M}\right) & for \quad M < \cos\theta \\ \theta - 90^0 & for \quad M = \cos\theta \\ \theta - \arctan\left(\dfrac{\sin\theta}{\cos\theta - M}\right) - 180^0 & for \quad M > \cos\theta \end{cases}. \qquad (6)$$

From Fig. 3 it is evident that the upstream ultrasonic beam drift is typically more severe than the downstream beam drift. That is, for the same Mach number, the absolute upstream beam drift angle is larger than the downstream beam drift angle. The flowmeter is eventually limited by the upstream signal when it comes to measuring extremely high flows [4]. The upstream signal is decreased by

about 6 dB due to the beam drift alone at a flow of around 100 m/s in air, while there other adverse effects imposed by the high flow, such as high flow noise and Doppler shift [14].
A recovery angle can be implemented to offset the beam drift effect, as demonstrated in Reference [5], where recovery angles were applied to both downstream and upstream transducers. It should be noted that the accurate implementation of recovery angle on both transducers could be either time consuming, particularly in the field during the hot/cold tap procedures, or costly, or both. Since the above calculation shows beam drift is primarily on the upstream signal generated by the downstream transducer, we implement the recovery angle on the downstream transducer by rotating it about 6^0 in favour of the high flow velocity. Here 6^0 is chosen as a compromise between high-flow and low-flow measurements.

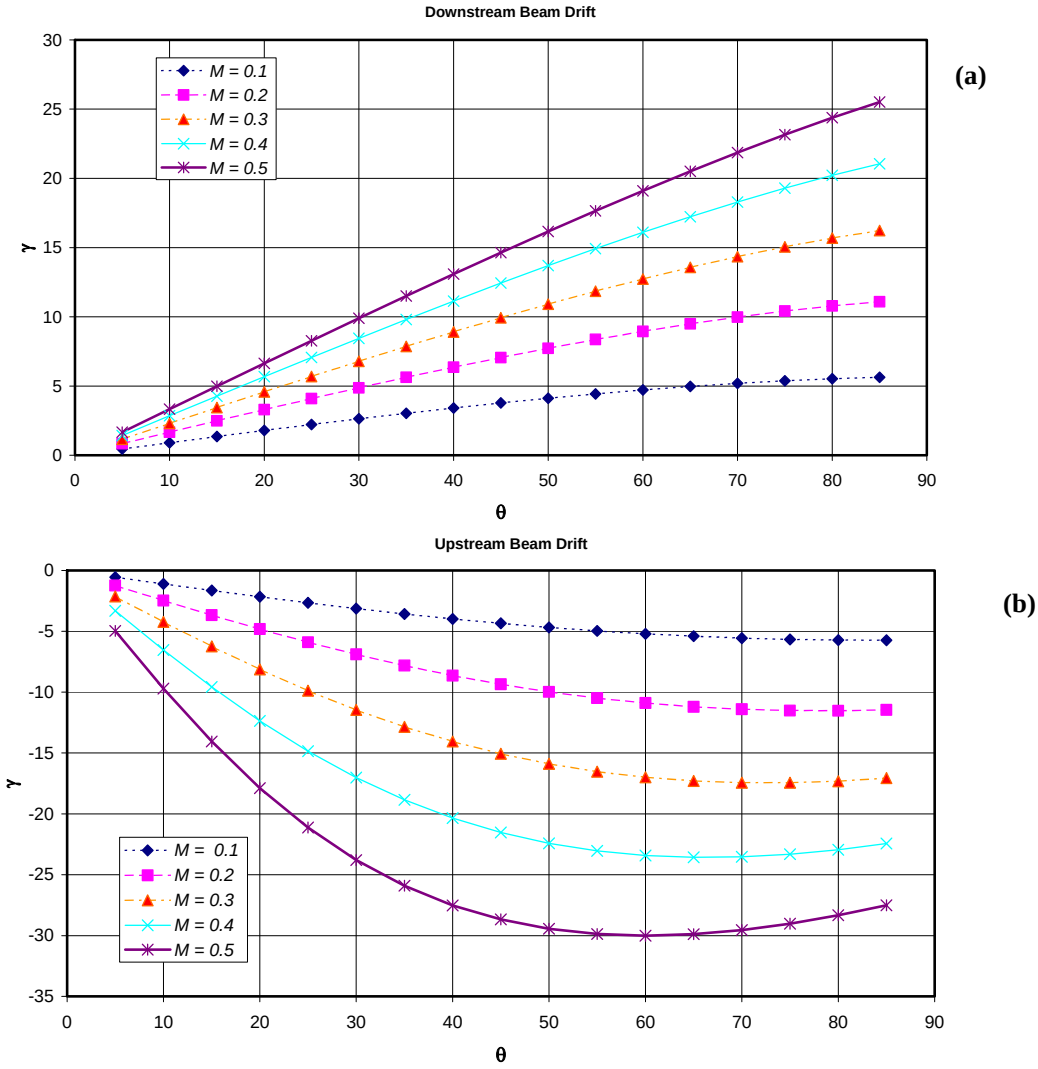

Figure 3. (a) Downstream and (b) Upstream ultrasonic beam drift angle as a function of ultrasonic path angle at different Mach numbers.

2.3 Increasing SNR

Another method we use to increase the SNR is to electrically tune the transducer. This is common for transducer design, and has been abundantly discussed in literature and thus omitted here for conciseness.

2.4 Final Conceptual Design

The final conceptual design of the high velocity flare gas ultrasonic meter is schematically shown in Fig. 4. The path length between transducers is kept relatively short, about 6 to 7.8", the path angle is chosen to be about 45^0, and the 6^0 recovery angle is implemented to the downstream transducer only. Two steel flow cells were manufactured for testing based on the above design. One is called Bias 90 (refer to Fig. 5 (a)) where the two transducers are placed on the same side of the flowcell, and the other is called Diagonal 45 (refer to Fig. 5 (b)) where the two transducers are placed from two different sides of the flowcell. It should be noted the transducers are rigidly mounted to withstand vibration, and that testing and calculation have shown the system to endure up to 120m/s and well beyond.

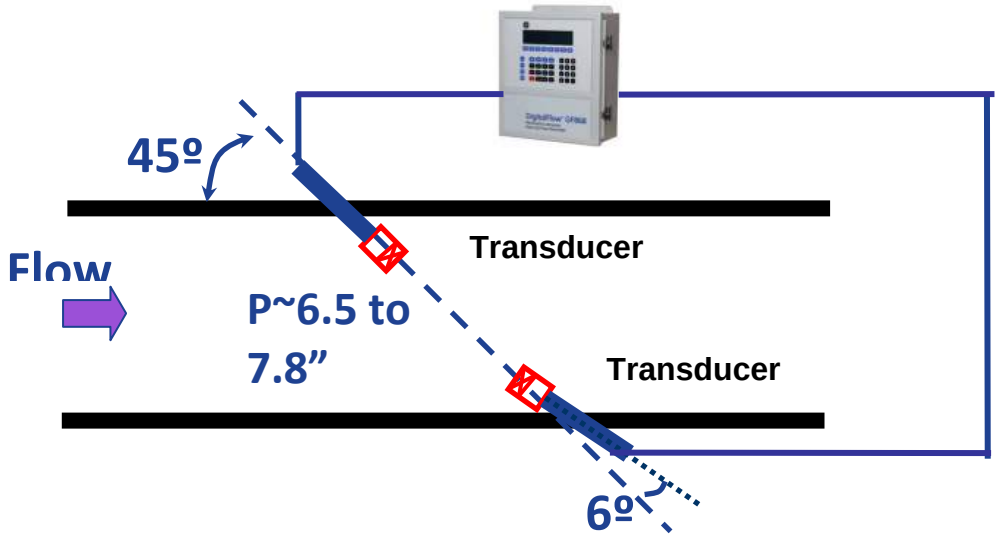

Figure 4. Conceptual design of the flare gas ultrasonic flowmeter.

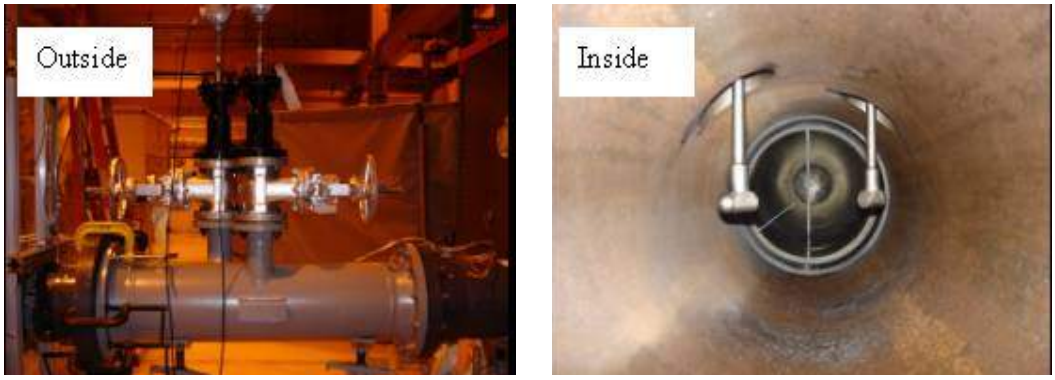

Figure 5 (a). Pictures of the Bias 90 carbon steel flowcell with transducers mounted, outside and inside views.

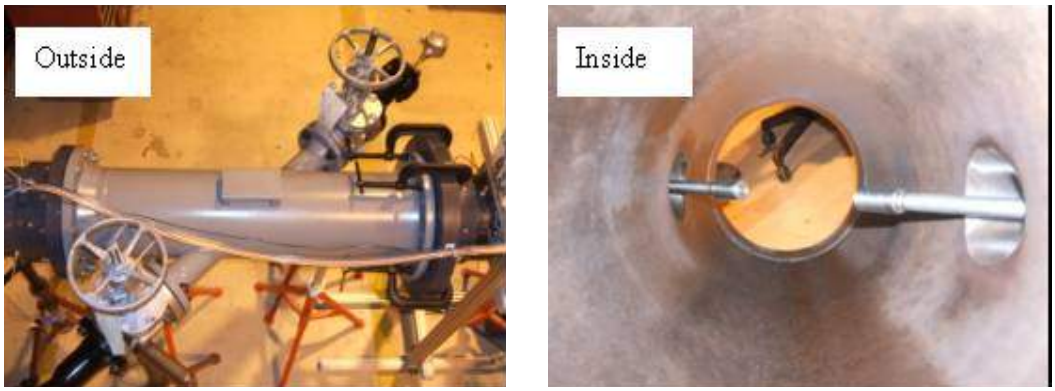

Figure 5 (b). Pictures of the Diagonal 45 carbon steel flowcell with transducers mounted, outside and inside views.

2.5 Testing Facility

Flow testing was performed in the Energy and Propulsion Technologies Laboratory at the GE Global Research Center (GRC) located in Niskayuna, NY in November 2008. Fig.6 shows the overall layout of the testing facility. Air was supplied by an open circuit high mass flow system, which consists of a three stage centrifugal blower, capable of 0 to 20,000 scfm, with 16-inch piping and multiple control valves. An inline Venturi tube was utilized to measure the flow. The 16-inch piping gradually expands into a plenum, upon which the test apparatus is attached. Perforated screens inside the expansion and plenum ensure uniform flow.

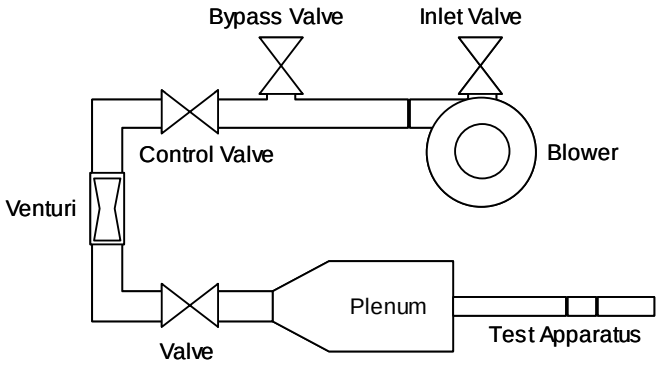

Figure 6. Illustration of open flow system at GE GRC.

2.6 Test Results

Fig. 7 shows the flow readings from the meter (called GF868) in comparison with the GRC reference readings, for the Bias 90 configuration and the Diagonal 45 configuration, respectively. As seen our meter readings agree with the reference readings very well across the velocity range of 31.2 m/s up to 123.7 m/s.

The percentage errors for both Bias 90 and Diagonal 45 configurations are within 2% across the velocity range of 31.2 m/s up to 123.7 m/s. With the reference accuracy of 1-2% (dependent upon the flow velocity range, refer to Appendix for details), we can conclude that the overall meter accuracy is better than 3-4%.

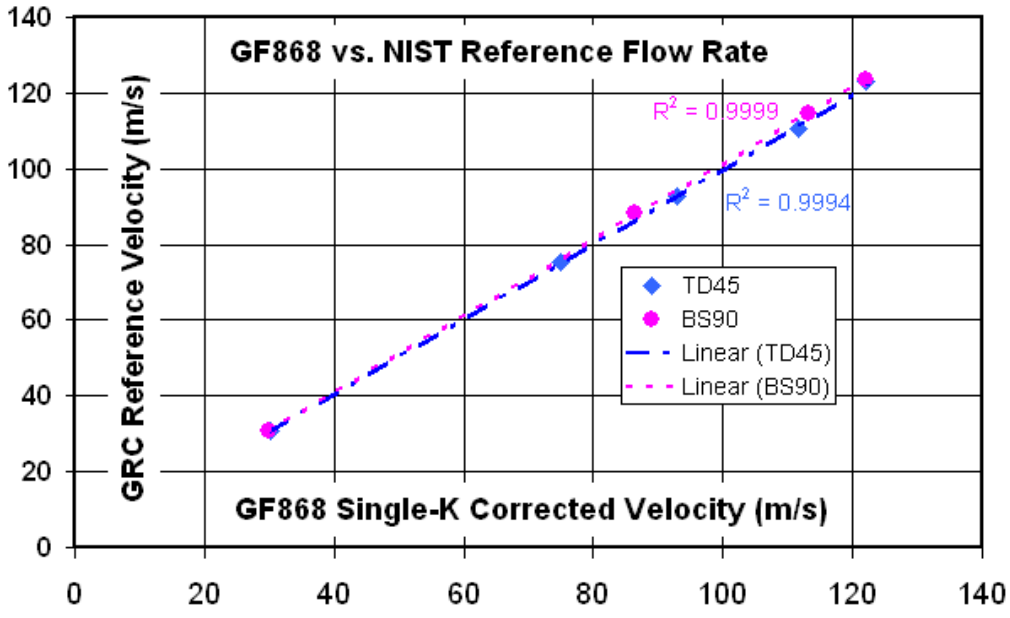

Figure 7. Flare meter reading in comparison with GRC reference reading for the Bias 90 configuration (BS90) and the Diagonal 45 configuration (TD45).

3 HIGH CO2 CONTENT FLOW MEASUREMENT

The flow rate of Flare Gas with a high concentration of Carbon Dioxide is becoming an important measurement for the petrochemical industry. In fact very new legislation for monitoring of Green House Gases has been issued by the EPA in the USA under 40CFR *Mandatory Reporting of Greenhouse Gases (GHG); Final Rule.* Flare gas monitoring for calculating CO2 emissions is mandated under Part 98 and covers petrochemical facilities. The EU has had directives for reporting of GHG for sometime now

3.1 CO2 Attenuation

CO2 is known to have an attenuating effect on ultrasound, and this can add to the already challenging flow measurement of flare gas with an ultrasonic flowmeter. The attenuation of CO2 has been known for quite some time and is comprised of two main components. There is classical attenuation simply due to density and distance between transmitter and receiver, and then there is the Relaxation effect due to the nature of the CO2 molecule. The primary illustration of these attenuation effects is seen in the chart below [16], see fig. 8.

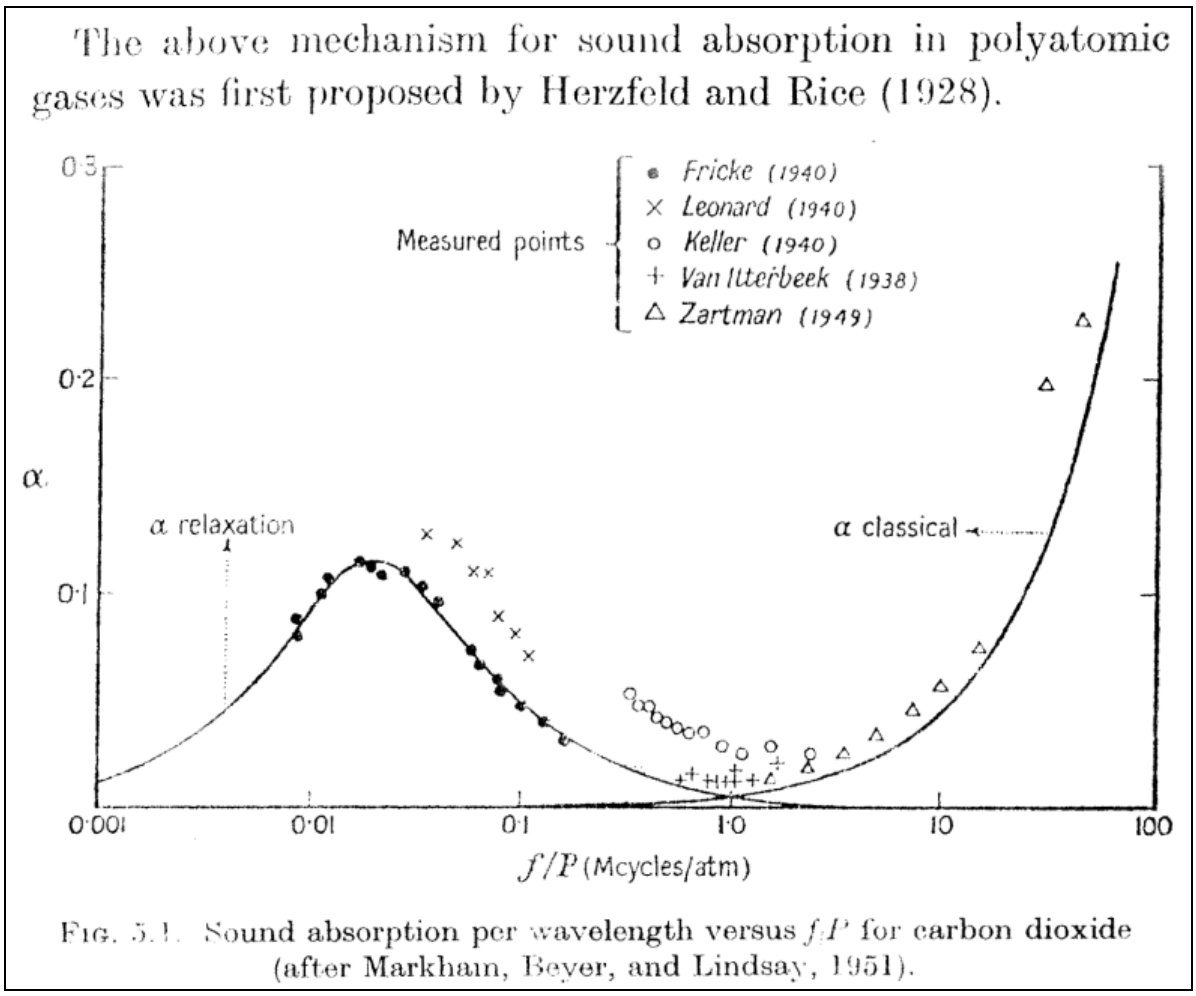

Fig. 8 Classic and Relaxation Effect attenuation in CO2 from [16]. Note Relaxation is directly proportional to frequency, yet inversely proportional to pressure

Original testing by us (Panametrics) was done with the then Exxon Co. back in the early 1980's in Baytown, Texas as part of the development of the Flare Gas Flowmeter. Shown here is a set of data collected from various gases including CO2 and other flare gases from 1982.
This testing as well as implementation of the Flare Gas flowmeter into working flare lines showed that while CO2 gas was attenuating, it was not overly difficult to still make flow measurements.

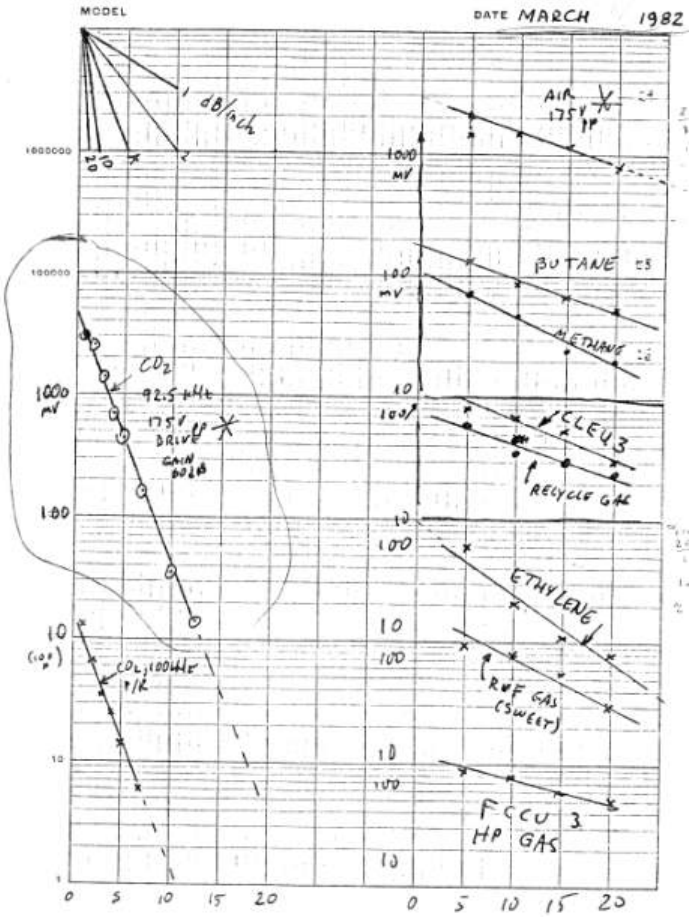

Fig. 9 Original plot of different flare gases' attenuation

Test	Test results		
MOLECULAR WEIGHT MEASUREMENT			
gas/gas mixture	True M.wt g/mole	Output error, % reading display	current
100% methane	16.04	- 8.0	- 7.2
100% n-butane	58.12	+ 5.8	(note 1)
50% ethane, 50% nitrogen	29.04	- 5.9	- 5.6
50% ethane, 50% nitrogen	29.04	+ 4.2*	+ 4.8*
100% ethane	30.07	- 0.7	- 0.5
50% ethane, 50% carbon dioxide	37.04	- 5.6	- 5.2
85% ethane, 15% nitrogen	29.76	- 2.0	- 1.7
85% ethane, 15% nitrogen	29.76	+ 2.3*	+ 2.8*
85% ethane, 15% carbon dioxide	32.16	- 2.0	- 1.6
98% ethane, 2% carbon dioxide	30.35	- 0.8	- 0.5
98% ethane, 2% nitrogen	30.03	- 0.8	- 0.4
98% ethane, 2% nitrogen	30.03	- 0.2*	+ 0.2*
50% methane, 50% n-butane	37.08	+ 2.2	+ 2.6
	note 1: no result given as the output was out of range and limiting.		

Additional testing by an independent organization, SIREP, was conducted in 1995. The data here shows the performance of the Flare gas flowmeter with varying compositions, many with a high CO2 content.

Fig. 10 Independent testing of an early flare gas flowmeter included CO2 mixtures.

3.2 Solutions

An in-house laboratory study of the CO2 attenuation effect was conducted in 2005 to model the effects on ultrasound. The volume fraction of CO2 in N_2 was modelled.

Model

Assume a measurement model as shown in Figure 11 where one transmitting transducer transmits acoustic waves into acoustic medium (here a mixture of CO_2 and N_2) and one receiving transducer receives those waves.

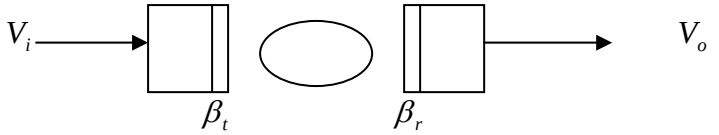

Figure 11. Measurement model

The receiving voltage from the measurement model can be written as

$$V_o = V_i \beta_t C A \beta_r \tag{7}$$

where

V_o is the output voltage

V_i is the input voltage

β_t is the transmission efficiency factor

C is the diffraction coefficient (reflecting beam spreading effect)

A is the attenuation of the medium

β_r is the receiving efficiency factor

The model uses transducers that are 100kHz type. We fix transducer size, distance, temperature, and pressure. Then physically if we only consider the terms that are possibly associated with gas components we have

$\beta_t \propto \rho c$ (proportional to acoustic impedance of medium)

$C \propto \frac{ka^2}{D} \propto \frac{1}{cD}$ (proportional to the inverse of distance)

$A \propto e^{-\alpha D}$ (attenuation in the exponential form)

$\beta_r \cong \text{constant}$ (transmission through a rigid body)

where

c is the sound speed in the gas mixture

D is the distance between the two transducers

α is the attenuation factor

Here we only focus on the attenuation change versus fraction change of CO_2 in N_2. Combining the above four terms yields

$$V_o / V_i \propto \rho e^{-\alpha D} \tag{8}$$

For our very specific problem, from the above equation, we can see that the signal strength is only associated with the density and attenuation factor of the gas mixture.

Density consideration

For a mixture of CO_2 and N_2, assume the fraction of CO_2 is *F*. Then the density of the mixture is expressed as

$$\rho = \rho_{CO_2} * F + \rho_{N_2} * (1 - F) \tag{9}$$

where ρ_{CO_2} is the density of CO_2 and ρ_{N_2} is the density of N_2.

Attenuation consideration

The attenuation factor is non-dimensionalized by the wavelength, or $\alpha\lambda$ is given instead of α itself. Then we need to consider the following expression,

$$\alpha = (\alpha\lambda)\frac{1}{\lambda} = (\alpha\lambda)\frac{f}{c} \tag{10}$$

where *f* is the frequency (=100kHz here). The sound speed is written as

$$c = \sqrt{\frac{\gamma RT}{M}} \tag{11}$$

where

$\gamma = \frac{C_p}{C_V}$ is the adiabatic constant

T is temperature in Kelvin (here we take *T*=298.15K)
R = 8.314 J/mol/K
M is the molecular weight of gas

By considering the fraction of CO_2 in the mixture, we have

$$\gamma = F * \gamma_{CO_2} + (1 - F) * \gamma_{N_2} \tag{12}$$

and the molecular weight

$$M = F * M_{CO_2} + (1 - F) * M_{N_2} \tag{13}$$

Via Eqs. (11), (12) and (13), we see that attenuation is a function of the fraction of CO_2 in N_2.

Simulation

From [13], the attenuation of CO_2 in N_2 was measured from 20% to 80% and is shown in Figure 12. This figure shows the dimensionless $\alpha\lambda$ versus frequency divided by pressure. This is called the attenuation spectrum.

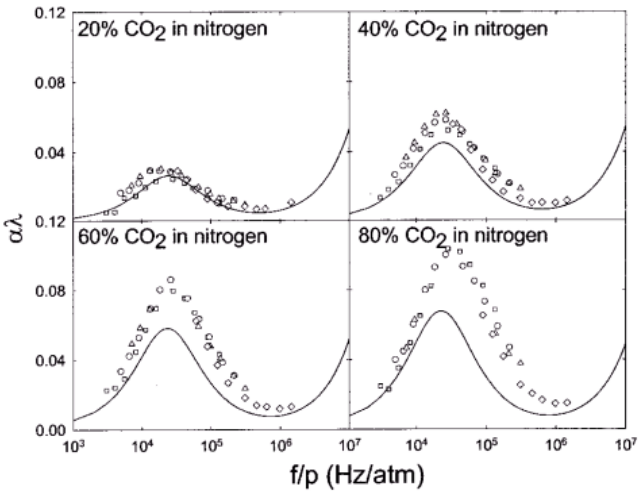

FIG. 10. Results for mixtures of 20%, 40%, 60%, and 80% CO_2 in nitrogen with the Pinkerton diffraction correction at average temperatures of 292.6, 293.7, 293.5, and 294.0 K, respectively. Data points are for the 92 kHz, 149.1 kHz, 215 kHz, and 1 MHz transducers (squares, circles, triangles, and diamonds, respectively). The solid curves are the calculations based on the vibrational relaxation model of Dain and Lueptow (Ref. 3) summed with the classical and diffusional attenuation.

Figure 12. Attenuation with CO2 in N2 from [17].

Here we only consider the case where *p*=1atm and thus the X-axis is the frequency. Extracting the values of $\alpha\lambda$ at 100kHz (10^5) in the four subplots we then fill them into the following table.

Table 1 - Measured data at 100kHz and 1atm

Fraction of CO_2 in N_2	Attenuation ($\alpha\lambda$)
20%	0.0125
40%	0.036
60%	0.052
80%	0.08

In the table, we only have four data points. Using linear fit, we obtain

$$(\alpha\lambda) = 0.10925 * F - 0.0095 \quad (14)$$

This equation is only valid from 20% to 80% of CO_2 in N_2. Then Eq. (8) is rewritten as

$$V_o / V_i \propto \rho e^{-(\alpha\lambda)\frac{Df}{c}} \quad (15)$$

Substituting Eqs. (9), (11) and (14) into Eq. (15) gives the relationship of the signal strength to the fraction of CO_2 in N_2.

Figure 13(a) illustrates the signal strength change with the fraction of CO_2 in N_2. This change only has relative significance. Figure 13(b) illustrates the linear trend of the signal strength in terms of dB with respect to the strength at 20%. From Figure 13(b) we could see that the signal strength is reduced by about 7.2dB when the CO2 is increased by 10%.

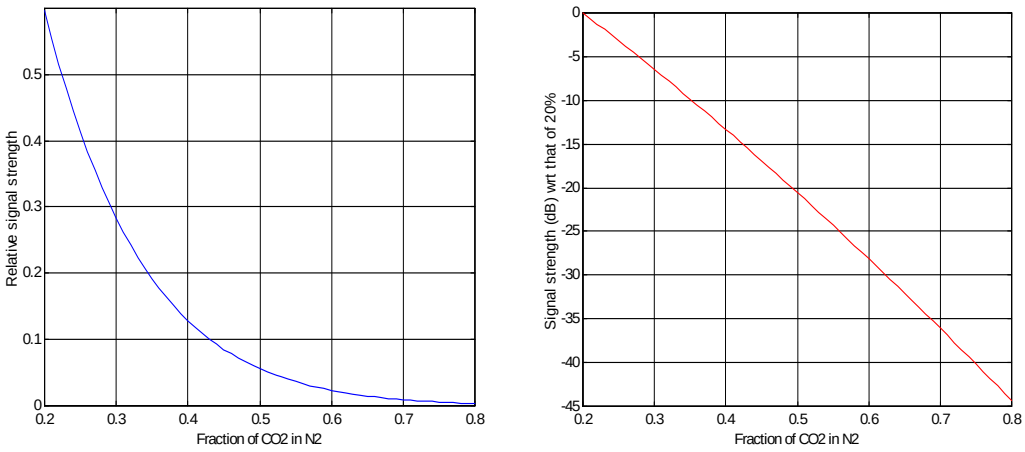

(a) (b)

Figure 13. Simulation

Transducer

To help avoid the highest attenuation from the Relaxation effect, and even from classical attenuation. The flare gas flowmeter can use a variety of ultrasonic frequencies for the transducer. The most common frequency is 100 kHz as used in the model above. The next lower frequency is 50 kHz, and because of its longer wavelength it is also a larger transducer. On some occasions higher frequencies are called for with 200 kHz being common, and 500 kHz rare, but possible. One major feature that differentiates one transducer from another is the power of the transducer designed and used. A more powerful transducer can overcome these forms of attenuation even at non-optimum frequencies.

Fig. 14 A variety of ultrasonic transducers, at different frequencies, are used in flare gas flow measurement.

3.3 Performance Test

In 2009 through 2010 we conducted testing for performance or accuracy impact from CO2 content in gas compositions. [19] Testing was done with the CTF878 gas clamp-on flowmeter, which has the following specifications:
Velocity Accuracy: 2% of reading
Repeatability: 0.6% of reading
Range ability: >100:1
Gas pressure: tested from ambient to 100bar
Gas temperature: tested from subzero to 450^{O}F
Pipe size: ϕ 2" to ϕ 30"
Turbulent flow only.
The CFT878 uses ultrasound to make flow measurement in steel pipes using the Tag Correlation method at frequencies of 200 to 500 kHz.

A baseline performance test was done on the same high velocity air flow loop at GRC in 2009 shown in fig. 15.

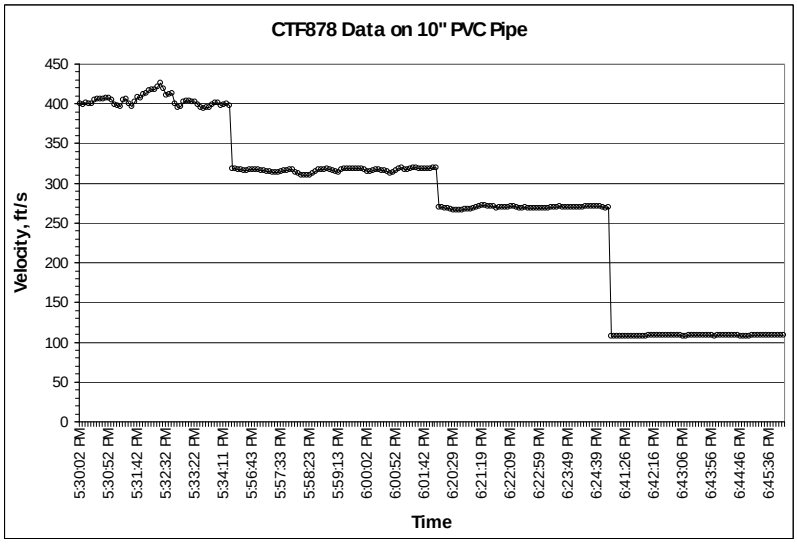

Fig. 15 CTF878 on 10" PVC pipe tested over full velocity range at GRC

The accuracy of the flow meter against the reference flow is plotted below in fig. 16.

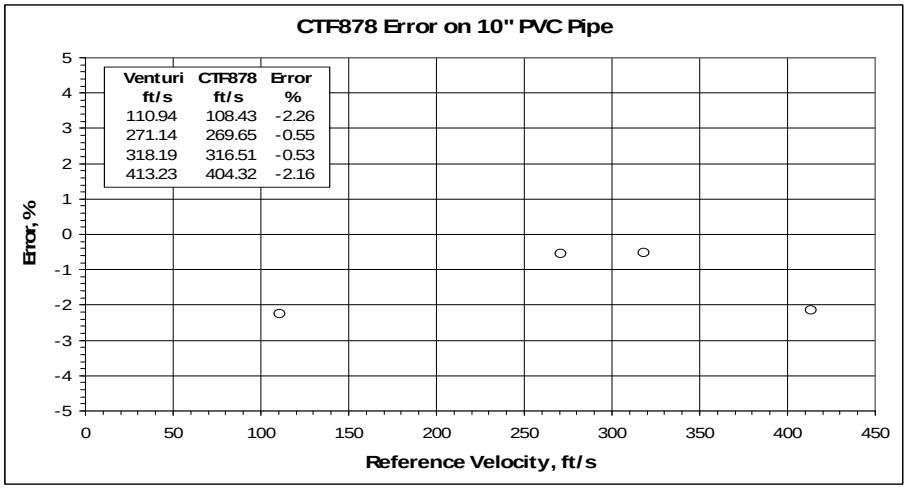

Fig. 16. Accuracy plot of clamp-on flowmeter velocity vs. the GRC reference.

The clamp-on meter was then compared to a reference flowmeter at a flow loop at the author's laboratory using various mixtures of CO2 with air. See fig 17 below for flow loop illustration.

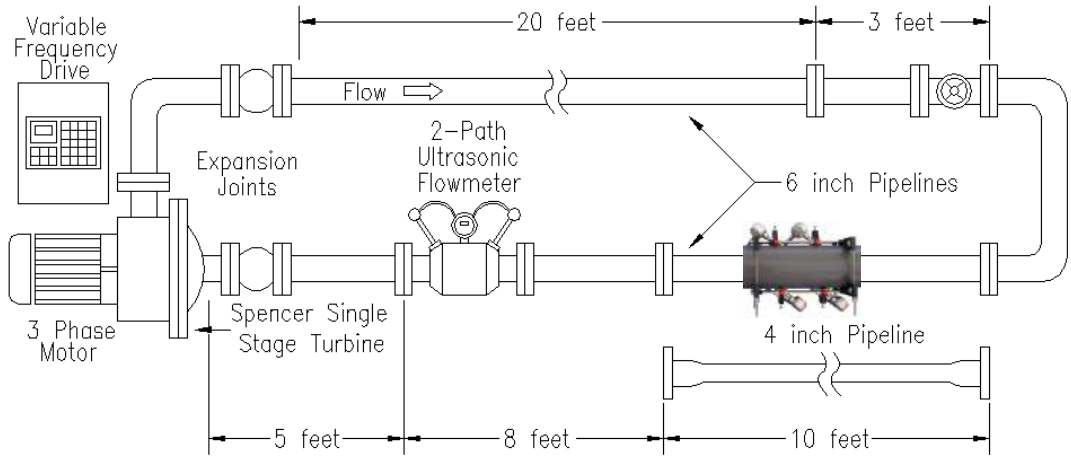

Fig 17 Compressed air loop, gas pressure up to 100psig and velocity up to ~120ft/s with CO2 mixtures.

As shown in fig 18 below, the relative accuracy of the flowmeter is unchanged for the various mixtures of CO2 with air, even at different pressures. No additional error is introduced with up to 30% CO2 within the meter specification Influence of CO2 on flow measurement in larger pipes (>12") or at higher pressure is expected to be even smaller when lower frequency transducers are applied.

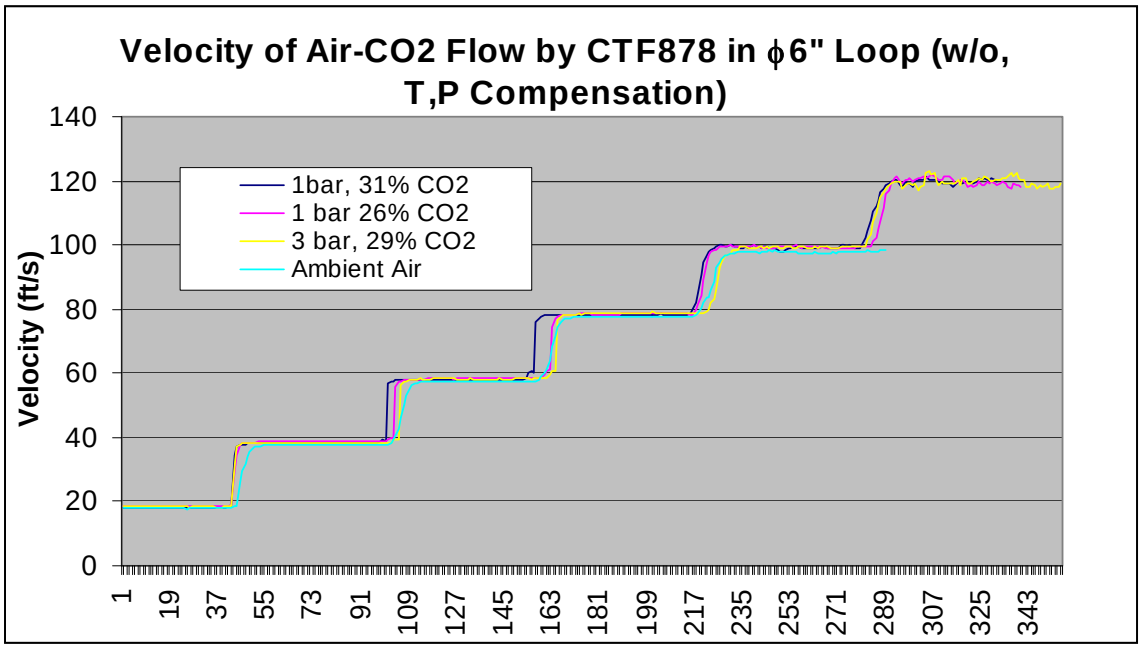

Fig 18. Accuracy of flow measurement is unchanged for various mixtures of CO2 with air at various pressures.

3.4 Application Review

To have a successful application with an ultrasonic flowmeter in gas streams with CO2 content it is required to review the conditions of the application to see if the ultrasonic frequency is right and to adjust the path length if necessary. Plotted below are some actual applications at different pressures, and other process parameters. The data put together here show that by avoiding the peak attenuation of the Relaxation effect the Ultrasonic Gas Flow Meter is quite capable and reliable over a wide variety of CO2 content, pipe size and pressure, see Table 2.

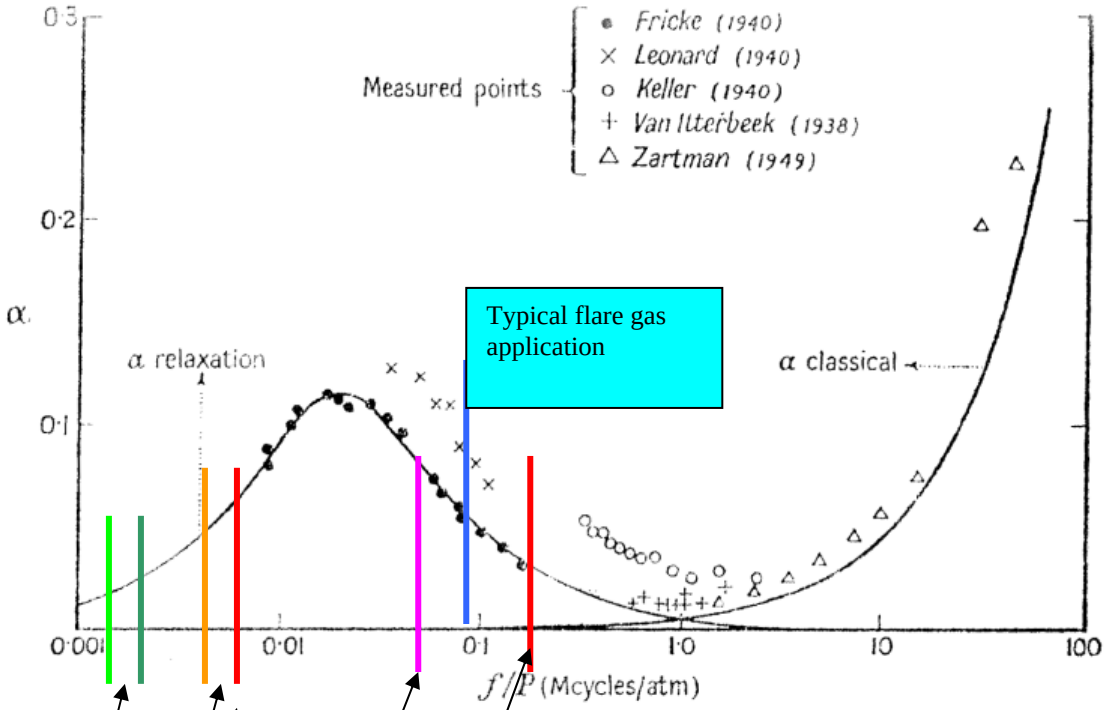

Fig. 5.1. Sound absorption per wavelength versus f/P for carbon dioxide (after Markham, Beyer, and Lindsay, 1951).

Application	Press (barg)	Press (atm)	Temp. (degree C)	CO_2 mole%	Mcycles/atm
XGM with 200 kHz BWT	1.39	1.372	185	78.5-90	0.146
XGM with T14	1.59	1.57	65	78.5-90	0.063

Application	Min Press (barg)	Max Press (barg)	Temp. (degree C)	Pipe Size (Meter Size)	Flow Rate (MMSCMD)	CO_2 mole%	Mcycles/atm (100 kHz)/ min P	Mcycles/atm (100 kHz)/ max P
AI	15	20	22.28	DN450	4.543	20%+	0.0067	0.005
B,C,D	40	60	22.61	DN400	3.936	20%+	0.0025	0.00167
E,F	15	20	30.01	DN250	1.343	20%+	0.0067	0.005

Fig. 19 Some actual field applications plotted on the attenuation curves at 100 kHz.

Table 2 - Process Applications with CO2

Application	Natural Gas Transport	Process	Process	Process	Coke Oven Gas (COG)	COG	COG	Steel (LDG)	Flue Stack	Process BFG (Flue)	Blast Furnace Gas	Flare	Flare-CO2 Recovery Injection	Flare
Qty/Size	9	24"	1 x 14"	1 x 400mm	1	1 x 40"	1 x 40"	1 x 1829 mm	6.34 meter	1	1 x 40"	1 x 24"	3 x 12-24"	1 x 36"
Location	Kazakhstan	Wyoming, USA	California, USA	East Europe	Asia	Japan	Japan	Japan	Spain	Asia	Japan	Texas, USA	Texas, USA	Wyoming, USA
User	IHC/SBM	ExxonMobil	Exxon	----	----	----	----	----	----	----	----	----	Oil co.	Amoco
Install date	2005	2004	2003	<2009	2007	<2008	2008/2009	2009	2005	2007	2008	2008	~1995	1994
Pressure	28 bar	(600#)	2.04 bar	1.08 bar	1.039 bar	1.045 bar	1.196 bar	1 bar	1 bar	1.078 bar	1.062 bar	1.55 bar	1-1.3 bar	1 bar
Composition														
Methane	51.076	1.5			26.6		29.2					1.4		
Nitrogen	0.562	3		48	2.3		3.4	18.1	71.8	54.1				
Ethane	10.785						2.3					0.82		
Propane	5.335											0.62		
Iso-butane	0.765													
N-butane	1.511													
Iso-Pentane	0.401													
N-pentane	0.394													
CO2	**5.649**	**69**	**100**	**7**	**3.1**	**2**	**2.1**	**16.4**	**14.2**	**20.7**	**23**	**97.16**	**85-90**	**>95**
CO				22	8.4		6.1	64.6		22				
H2S	22.076													
Hydrogen		12		18	56.4		56.4	0.9		3.2				
Hexane														
C6+	0.65													
H2O	0.796			5					10.88					
Other		14.5			2.9	98	0.5				77		15-Oct	<5
Oxygen					0.3				3.12					

Fig. 20 This installation is on a 14 inch pipe, with a 19 inch path. In 100% pure CO2. Temperature is ambient and pressure approximately 30 PSIA. Plot of freq/pressure =0.05 with a 100 kHz transducer is shown.

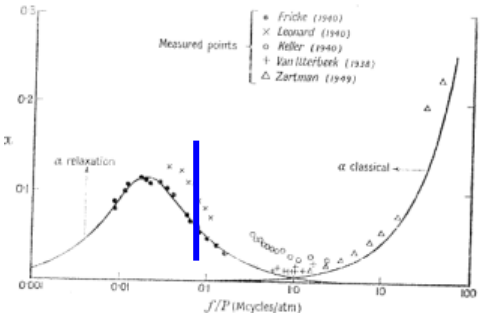

4 LOW VELOCITY FLOW

Regulations on emissions in North America, Europe, and even Asia, around Green House Gases and other materials have made petrochemical facilities with Flares look closely at low flow velocities. Users and Regulators are realizing that continuous low flow can add up to significant quantities of gas. Stack emissions allocations can be reached with low flow, and not just with relief flow rates.
The low flow regime is typically from 0.03 to 0.3 meter/second (0.1 to 1 feet/second) in terms of velocity.
Current accuracy requirements at these low flow velocities is not always well defined by regulations, but is typically given as +/-20% at and below 0.3 m/s. However the trend is for better: to 5%.
In some regions the flare stack is given, or allocated, a total amount emissions it can produce in a time interval, typically a year. More accurate measurement of this low flow will allow users to operate longer before these allocation limits are exceeded.

4.1 Two Part Challenge

The flow velocity in flares is often in the range below 0.3m/s, but it is important that we look towards ways of improving the measurement accuracy over that range of velocities but still make a measurement at the high end of the velocity range during facility relief or upsets. Low flow presents two major challenges for the flow meter. Firstly is the resolution in velocity measurement by the meter itself, and secondly the asymmetric flow in the pipe where non-axial flow is on the same magnitude as axial flow.

4.1.1 Accuracy/Resolution at Low Flow

In the transit time ultrasonic flowmeter the measurement of time and distance determines the fundamental resolution in velocity. For the current meter the time measurement resolution is on the order of 50 nanoseconds (nS) at higher flow rates, and about 10 nS for lower flow rates. (The noise (SNR) at high flow limits the resolution).
The typical path length, or distance, is based on the installed transducer configuration. It is the projection of that path (L) in flowing fluid that directly affects velocity. The gas composition now enters the calculation since that determines the sound speed, and we use the following approximation to determine resolution in velocity:

$$V = \frac{\Delta t \bullet c^{2}}{2L} \qquad [16]$$

where

V_o is gas flowing velocity

Δt is resolution in time of the difference in transit times

L is axial projection of the path length in flowing fluid

c is the sound speed of the gas

For the Bias 90 configuration the most common path length is about 1.08 feet or 0.329 meter with an L of 0.233 meter. A common flare gas sound speed might be 410 m/s, and using 50 nS for time resolution we get a velocity resolution of 0.018 m/s. At a flow rate of .3 m/s this is about 6% inaccuracy, and at .03 m/s about 60% inaccuracy. However at low flow the meter will use the 10 nS resolution and the associated velocity resolution will be .0036 m/s. At 0.3 m/s this will calculate as inaccuracy of ~1.2%, and at 0.03m/s the inaccuracy shows as about 12%.
Actual inaccuracy will change if the gas composition produces a different sound speed, with higher sound speeds (i.e. hydrogen) increasing the inaccuracy.

For the Diagonal 45 configuration the same calculations hold true. As above the inaccuracy will depend on the path length, with longer paths lengths (an longer L) giving smaller values for velocity resolution and hence lower inaccuracy.
However there is a limit to how long a path can be since the attenuation of the ultrasonic signal is a function of the distance between transducers, as shown in section 3.2 above.

4.1.2 Asymmetric Flow

The second challenge of low flow is asymmetric, or non-axial flow velocity contributing to a significant degree to the transit times. The non-axial component of flow measurement is an error in the average flow measurement, unless it can be accounted for or eliminated.
Non-axial flow takes the form of cross flow or circulation. This can be induced by convection flow within the piping, or by stratification of different density gases within the total gas composition.

Convection generated cross or circulation flow may dominate over axial flow in magnitude at very low flow rates. A single path measurement may not be sufficient to eliminate or reduce this error. To illustrate this consider the following case of a large flare gas main header pipe at a Texas, USA facility. This flare line was instrumented with both a Bias 90 and a Diagonal 45 path configuration as shown in the figure 21 below:

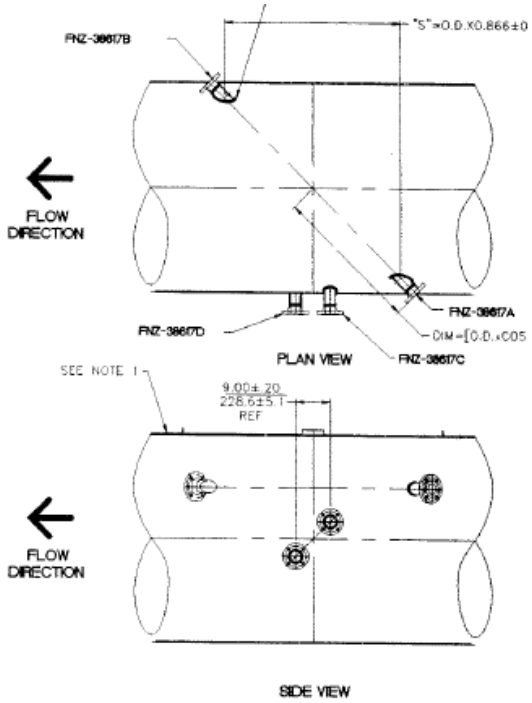

Fig. 21 Here we see two views of the transducer ports on this pipe. The Bias 90 set are close together, while the diagonal 45 set are virtually on opposite sides of the pipe. The diagonal 45 configuration is not on the diameter, but is an off-diameter path.

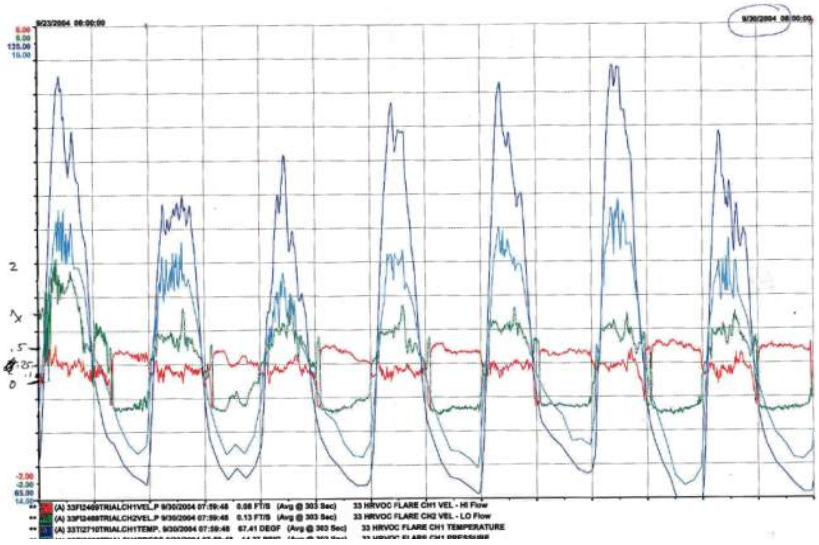

Fig. 22 Control room plot of the Bias 90 and Diagonal 45 flow rates along with pipe temperature and pressure. Showing the flow rate changes about 0.15 m/s on the bias 90, and from +0.3 to –0.3 m/s on the Diagonal 45 twice a day at about 8 am and 8 pm.

This behaviour can be explained by convection flow changing the direction of cross flow. As illustrated in the figure below it only takes a very small change in the direction of the cross flow to make the Diagonal 45 path appear as if the flow reversed direction, when in fact it did not. The Bias 90 path is not sensitive to this direction of cross flow, so it measures the axial flow alone.

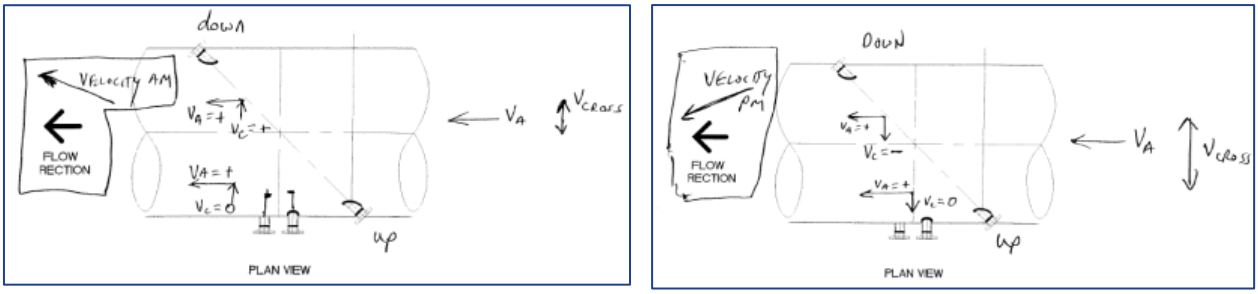

Fig 23 Schematic representation of the axial flow, Va, the cross flow, Vc and how a slight change in the cross flow direction can reverse the flow indication on the Diagonal 45 path, but not the Bias 90 path.

To verify the idea that convection flow can show these low flow effects, the ambient temperature of the city where the flow meter is located is plotted against the trend flow rate data for the same dates. In this case the match in unmistakable. See fig 24.

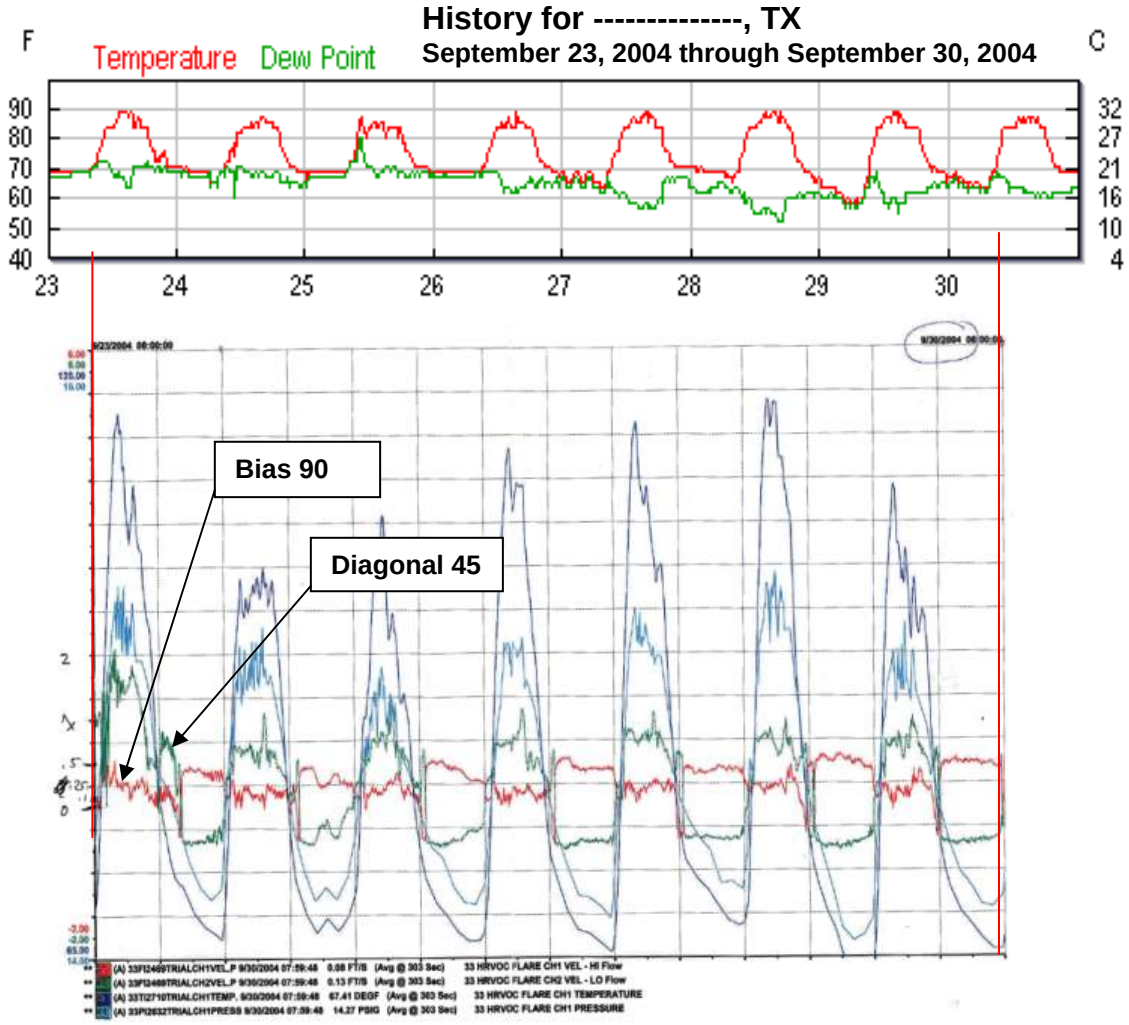

Fig 24 The historical temperature data for the location of the facility where the meter is located plotted against the observed flow rates form the two paths.

Convection flow as well as stratification is also exhibited on this 24" flare line where the meter is showing low flow peaks that also follow the ambient temperature. With up to 70% Hydrogen, by volume, possible in the pipeline, circulation flow seems to be present at the lowest flow rates where the different density gases can separate.

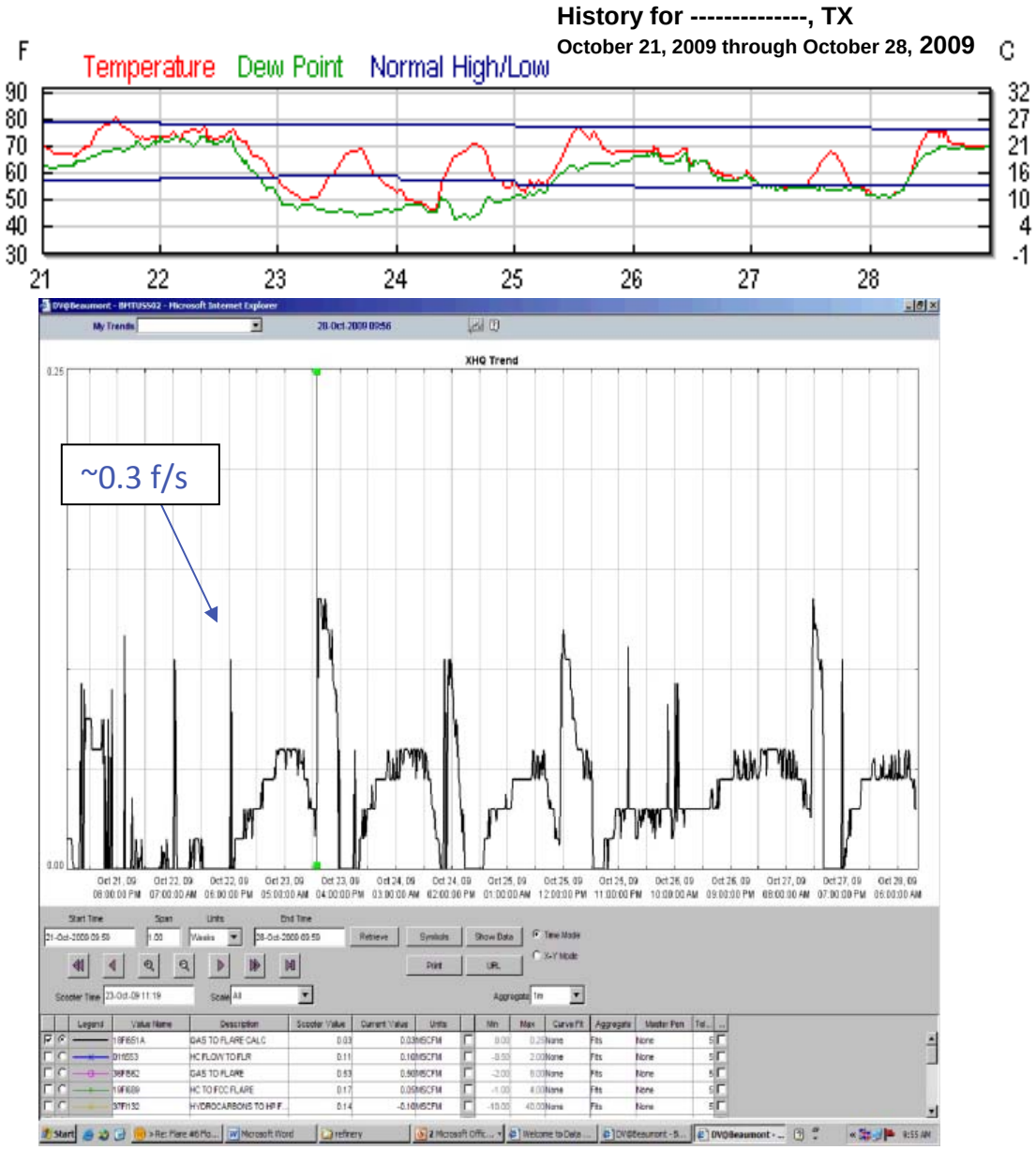

Fig 25 A 24" flare with a Bias 90 installation on the top of the pipe. Stratification and convection flow producing peaks of low flow based on the ambient temperature, but not evident at the flare tip.

4.1.3 Convection Model in CFD

To help verify the convection flow in the flare line we have applied CFD (Computerized Fluid Dynamics) to a model of convection flow. Fig. 26 shows the convection flow induced by a 20 C differential between top and bottom (or any opposite sides) of a circular pipe. Note flow rates from 0.09 to 0.3 m/s.

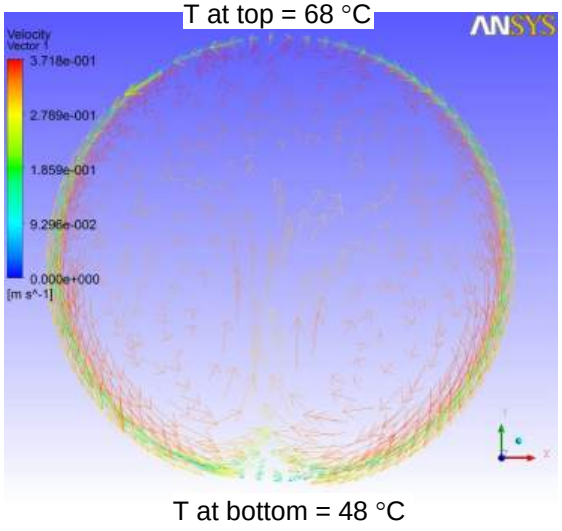

Fig 26 Convection flow of gas in a 24" pipe with 20 C temperature difference top to bottom.

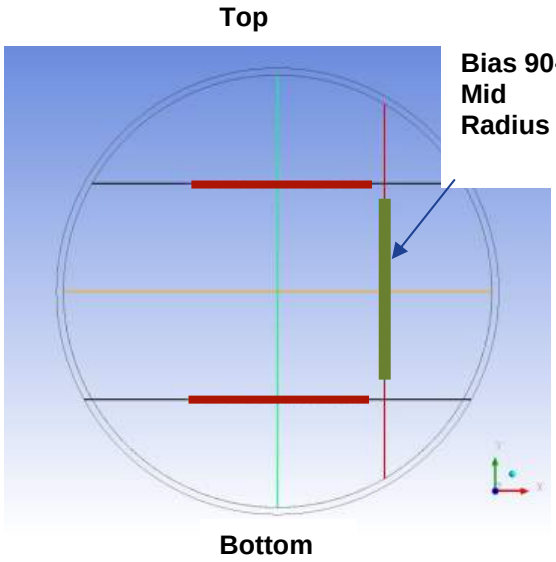

Fig 27 Diameter, Mid-Radius and bias 90 paths are modelled.

The results have demonstrated that the natural convection due to the temperature gradient from solar radiation is significant. [18]
Cross flow can be 8 to 15% of a 0.3 m/s (1 f/s) mean flow rate (Vm) at these very low velocities. It depends on path position, the actual mean flow velocity and the solar radiation absorption of the system.

	up/Vm	vp/Vm	wp/Vm	Vpath	k=Vm/Vpath
Dia X A	0.00047	0.00278	0.98401	0.29928	1.01577
Dia X B	0.00093	0.00126	0.98284	0.29850	1.01843
Dia Y A	-0.00019	0.15497	0.91371	0.32488	0.93574
Dia Y B	0.00026	0.15282	0.90984	0.23014	1.32096
Mid XR Y A	0.00108	-0.02912	1.04361	0.30840	0.98572
Mid XR Y B	-0.00029	-0.02698	1.04410	0.32561	0.93364
Mid YR X A	-0.00197	0.01076	1.11274	0.33767	0.90028
Mid YR X B	-0.00160	0.00739	1.11556	0.33962	0.89513
Mid negYR X A	-0.00251	0.00196	0.97434	0.29544	1.02899
Mid negYR X B	-0.00388	0.00515	0.97286	0.29693	1.02382
Mid XR Y A Bias	0.08211	0.00196	0.97434	0.29544	1.02899
Mid XR Y B Bias	0.08080	0.00969	1.01771	0.30644	0.99204
Mid YR X A Bias	-0.00083	0.06433	1.10599	0.33597	0.90485
Mid YR X B Bias	-0.00038	0.06344	1.10836	0.33706	0.90193
Mid negYR X A Bia	-0.01039	0.21559	1.00426	0.30213	1.00617
Mid negYR X B Bia	-0.01094	0.21737	1.00290	0.30821	0.98635

Fig. 28 Average velocities along various paths with area averaged Vm=0.304 m/s. u and v are cross flow component, while w is axial flow component.

4.2 Low Flow Solutions

Solutions for accurate low velocity measurement in the flare line entail using different approaches, based on the individual conditions. For improved resolution the basic choice is one longer path. This may meet the requirement, but it can depend on gas composition, pipe size and how the asymmetrical flow is formed.
Two or more paths are now a common solution to get the highest accuracy over the widest range of conditions. In many cases the system will use one path for high flow and one path for low flow. Figure 29 below illustrates the addition of a Diagonal 45 diametrical path to the existing Bias 90 path on the 24" pipe shown above. The result is improved performance at the low flow showing a better average of asymmetric flow, while maintaining the performance and accuracy at high flow even with high amounts (to 70 %) of hydrogen.

Fig. 29 24" flare line now with both original Bias 90 installation and with diametrical Diagonal 45 installation

The Diagonal 45 path will have longer path length, and resulting axial length, and will be able to measure the velocity with a greater resolution than the Bias 90 with it's shorter path. The Diagonal 45 path may be across the diameter, or unconventionally, at an off diameter location. The nozzle, or ports, for the transducers must be located to cause little or no interference with each other. See the illustrations below for examples of this. Alternatively the use of two Bias 90 configurations may provide sufficient accuracy improvement while allowing installation on flare lines with restricted access.

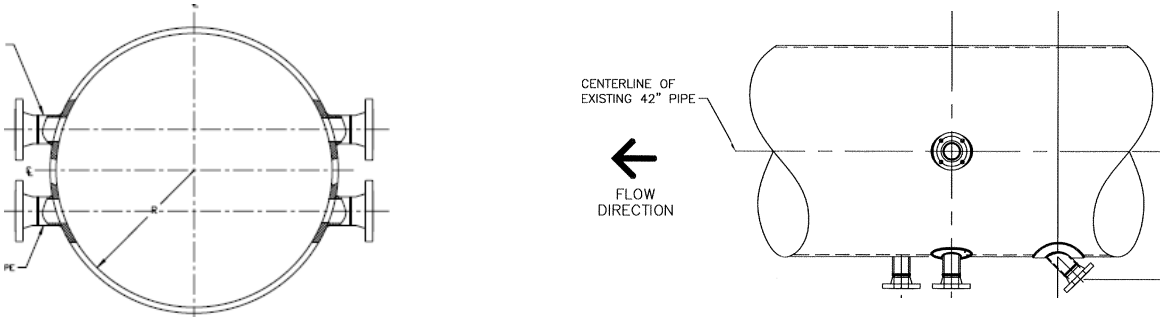

Fig 30 Left hand drawing shows two sets of ports for a two-path bias 90 installation. The right hand drawing shows Bias 90 ports with a second path in a "90-180" configuration. These systems can provide the accuracy required at low flow in difficult installations.

**Fig 31 Installed systems of two-path bias 90 (high flow) and a two-path Diagonal 45 (low flow).
Note separation of the two-path systems to avoid potential acoustic crosstalk**

5 CONCLUSION

In summary an ultrasonic flare gas flow meter has been developed to demonstrate the accurate measurement of air flow up to 123.7 m/s. Some of the new enabling technologies are detailed, primarily focused on the mechanical and transducer developments. Testing data have been presented for two typical configurations, Bias 90 and Diagonal 45, in comparison with a Venturi reference. The overall accuracy of the meter is shown to be better than 3-4% with reference meter uncertainty included, dependent upon the flow velocity range, and the relative standard deviation of our meter readings is within 1.2%. The new development could potentially translate into an even higher flow-velocity flare gas measurement, depending on the flare gas composition.
There is concern in the industry about the effects of CO2 on the ultrasonic flow meter's performance. While there is a specific effect due to the Relaxation effect of the CO2 molecule, it is dependant on parameters of frequency and pressure. This can be addressed with careful review of any application with appreciable CO2 content, and there have been many successful installations by selecting the proper transducer frequency and controlling the path length. The amount of CO2 mixed with other gases does not affect the accuracy of the volumetric flow rate measurement in the ultrasonic flowmeter.
Techniques of using longer path lengths, and two paths have been used to address the error seen at low flow, whether due to a need for improved resolution or to deal with asymmetric flow from convection flow or stratification.

6 APPENDIX: GRC REFERENCE UNCERTAINTY

All pressure and temperature measurements were made using National Institute of Standards and Technology (NIST) traceable instrumentation. At each velocity set point, a time delay preceded sampling to ensure flow stabilization. Each sensor would then be sampled for 10 seconds, at 10 measurements per second, and averaged for that point; this procedure was followed for all measurements. Each sensor was calibrated by NIST traceable calibration equipment prior to testing, in addition to manufacturer calibration. The uncertainty in the measurements varied by sensor type. For the static pressure sensors, the combined uncertainty, u_c, was +/–51.74 Pa, while the total pressure sensor u_c was +/–51.97 Pa. The Venturi measurement used pressure sensors with the upstream u_c equal to +/– 89.69 Pa and the throat u_c equal to +/–35.23 Pa. The temperature sensors used were standard type T thermocouples. The u_c values for the Venturi, stagnation chamber, and test section temperatures were +/–0.41 K, +/–0.42 K, and +/–0.41 K, respectively. The technique used to determine measurement uncertainty for the instrumentation is outlined in NIST Technical Note 1297 [15].
The u_c values were conservatively propagated through the velocity calculations for each measurement, and therefore varied at each velocity point. Typical velocity error for the profile measurements is less than 1.0%, with higher error values at the low velocities ($\leq$ 50 m/sec). Typical error for the reference velocity measurements is less than 2.0%, with higher error values at the low velocities ($\leq$ 50 m/sec). For example in uncertainty; the free stream velocity value of 120.6 m/sec +/–0.8 m/sec, and the reference velocity of 112.5 m/sec +/–1.8 m/sec.

7 REFERENCES

[1] J.W. Smalling, L.D. Braswell, L.C. Lynnworth, and D.R. Wallace, Flare Gas Ultrasonic Flow Meter, Proceedings from the Thirty-Ninth Annual Symposium on Instrumentation for the Process Industries, pp. 27-38,1984.

[2] D. Belock, How much do you flare?—How to measure flowrates of flare gas accurately and reliably, Process worldwide, Issue 3, pp. 18-19, 2006.

[3] NORWEGIAN PETROLEUM DIRECTORATE. Regulations to measurement of fuel and flare gas for calculation of CO2 tax in the petroleum activities, August 1993(ISBN 82-7257-395-4).

[4] L. Sui and T.H. Nguyen, Ultrasonic Flow Meter, US Patent Application No.12272174 filed in November, 2008

[5] K.S. Mylvaganam, High-rangeability ultrasonic gas flowmeter for monitoring flare gas, IEEE Transactions on Ultrasonics, Ferroelectrics and Frequency Control, Vol. 36, pp. 144-149, 1989.

[6] GE Sensing, GF868 Brochure, http://www.gesensing.com/downloads/datasheets/920_009c.pdf

[7] O. Rutten, Deutsches Patent No. 520484, 1928.

[8] L.C. Lynnworth, Ultrasonic Measurement for Process Control: Theory, Techniques, Applications, Academic Press, 1989.

[9] ANSI/ASME MFC-5M-1985, “Measurement of Liquid Flow in Closed Conduits Using Transit-Time Ultrasonic Flowmeters”, An American National Standard, 1994.

[10] M.F. Hamilton and D.T. Blackstock, Nonlinear Acoustics: Theory and Application, Academic Press, 1998.

[11] L.E. Kinsler, A.R. Frey, A.B. Coppens and J.V. Sanders, Fundamentals of Acoustics, John Wiley & Sons, 3rd Ed., pp. 179,1982.

[12] FUNDAMENTALS OF ELECTROACOUSTICS, http://www.massa.com/fundamentals.htm

[13] L.C. Lynnworth, D.R. Patch and W.C. Mellish, “Impedance-Matched Metallurgically Sealed Transducer, IEEE Transactions on Sonics and Ultrasonics, Vol. SU-31, pp. 101-104, 1984.

[14] P.M. Morse and K.U. Ingard, Theoretical Acoustics, Chapter 11, Princeton, 1986.

[15] B.N. Taylor and C.E. Kuyatt, *Guidelines for Evaluating and Expressing the Uncertainty of NIST Measurement Results*, NIST Technical Note 1297, 1994.

[16] Markham, Beyer and Lindsay "Review of Modern Physics" 23**,** 353 .(1951)

[17] SG Ejakov, S Phillips, Y Dain, RM Lueptow, and JH Visser, “Acoustic attenuation in gas mixtures with nitrogen: Experimental data and calculations”, JASA 113(4) Pt1 1871-1879.

[18] L. Shen, PhD, “Numerical Simulation for Low Velocity Air Flow Exposed to Solar Radiation”, GE Sensing report, pp. 1-12, 2010.

[19] S. Ao, PhD, J. Matson, O. Khrakovsky, “Wetted and Clamp-on Gas Flow Meter under Harsh Conditions”, GE Sensing report, pp 21-25, 2010.

North Sea FLOW Measurement Workshop

Paper 3.2

Calculation of the Uncertainty in the CO_2 Emissions Factor in Flare Lines with Nitrogen Injection

Jeff Gibson
TUV NEL

Richard Paton
TUV NEL

Pål Jaghø
Talisman Energy Norge AS

TÜV SÜD

nel technology for life

Calculation of the Uncertainty in the CO_2 Emission Factor in Flare Lines with Nitrogen Injection

Jeff Gibson, TUV NEL
Richard Paton, TUV NEL
Pål Jaghø, Talisman Energy Norge AS

1 INTRODUCTION

North Sea oil and gas operators are under both environmental and financial pressure to reduce CO_2 emissions from process and production facilities. Talisman Energy in Norway (Talisman Energy Norge AS) are reducing the amount of gas flared on their Gyda and Varg facilities using various process improvements. In order to do this a proportion of the fuel gas, used to keep the flare line pressurised and the flame burning during low-flaring conditions, is being replaced with injected nitrogen. This has the effect of reducing the CO_2 emissions.

Talisman have installed ultrasonic flare gas meters as the primary flow measurement devices in the flare lines on their Gyda platform. The output of molecular weight from the ultrasonic flare gas meters is being used to determine the composition and, hence, the CO_2 emission factor. Accounting for the gas flared, and therefore the CO_2 produced, requires measurement and calculation methods which account for the proportion of injected nitrogen. A similar system is proposed for the Varg FPSO.

Following an initial evaluation of the uncertainty calculations for emission factor undertaken in May 2009, TUV NEL was further commissioned to provide a calculation procedure to allow the CO_2 emissions to be reported from Talisman's Gyda and Varg platforms. This included an analysis of the flow-weighted mean emission factor for each of the flare lines. This paper focuses on the work done for the Gyda platform.

A review of the measurement and data collection/reduction methods was carried out, followed by an uncertainty analysis. A calculation spreadsheet was developed by TUV NEL in order to determine the emission factor, the CO_2 produced and the accompanying uncertainty over a specific reporting period.

This paper outlines the findings from the study expressed in a generic way in order to highlight the issues with measurements, data reduction and uncertainty that would apply equally to other operators' facilities. The analysis has highlighted that the measurement of the flare and nitrogen flow rates are of equal importance to the calculations of the emission factor as the algorithm used to calculate the molecular weight.

2 BACKGROUND

Gyda is a fixed oil production and drilling facility located in the southern-Norwegian sector of the North Sea. Gyda incorporates emergency flare systems which release CO_2 to atmosphere when this excess hydrocarbon gas is burned. Gyda has two flare lines, a high pressure (HP) flare and a low pressure (LP) flare. These flare lines are both injected with nitrogen to maintain a positive pressure on the flare whilst reducing the amount of gas burned and, therefore, the amount of CO_2 released to atmosphere.

Both the flow rate of gas to flare, and the appropriate CO_2 emission factor (tonnes CO_2 per tonne of gas flared), are required to calculate the amount of CO_2 emitted to atmosphere.

One method for determining an installation-specific emission factor is to obtain the gas composition by extracting samples for subsequent lab analysis. It is, however, generally impractical to extract samples from flare lines, mainly due to health and safety constraints. In most cases the only opportunity is to sample from the fuel (or export) gas line to give an estimate of the flare gas composition. This approach effectively ignores the variations in gas

composition that will occur during flaring incidents and does not directly account for the injected nitrogen.

An alternative solution is to use a combination of online molecular weight measurement from flare gas ultrasonic meters, in combination with sampling of the fuel gas, to determine the hydrocarbon content and percentage of inert gases in the mixture (such as CO_2, nitrogen (N_2), water vapour etc.). This is the approach that Talisman are proposing to use for determining the emission factor.

2.1 Regulatory Requirements

Gas flaring has been heavily regulated in Norway since the introduction of a CO_2 taxation regime in 1991. Norway also participates in the EU ETS through the incorporation of the EU ETS Directive 2003/87/EC (as amended) [1] within the European Economic Area (EEA) agreement. The requirements of the MRG are implemented at a National level by the Norwegian regulator of the EU ETS - the Climate and Pollution Agency (KLIF) (formerly SFT).

The EU ETS Measurement and Reporting Guidelines 2007 (MRG) Annex 2.1.1.3 [2] requires the mass of CO_2 released to atmosphere from flaring to be calculated via the product of the annual volume flared (referred to as the "activity data") (Sm^3), emission factor (tCO_2/Sm^3 of gas flared) and oxidation factor (-)

$$\underset{(tCO_2)}{CO_2 \text{ emissions}} = \underset{(Sm^3)}{\text{Activity data}} \times \underset{(tCO_2/Sm^3)}{\text{Emission factor}} \times \underset{(-)}{\text{Oxidation factor}}$$

Activity data (and emission factor) has to be based on specified standard conditions of the gas as defined in the EU ETS as 'normal' conditions of 1.01325 bar and 273.15 K (0°C).

It is noted that activity data and emission factor based on mass units is also widely accepted. Oxidation factor, a measure of the amount of CO_2 produced through burning, is generally specified as a constant (and is currently accepted as being set equal to 1).

The EU ETS MRG states that:

"The highest tier approach shall be used by all operators to determine all variables for all source streams for all Category B or C installations. Only if it is shown to the satisfaction of the competent authority that the highest tier approach is technically unfeasible, or will lead to unreasonably high costs, may a next tier be used for that variable within a monitoring methodology".

Gyda is a category B installation. Of note is the stipulation that activity data and emission factor are to be reported to the highest tier for both category B and C installations (i.e. flow rate and emission factor both to tier 3 as per category C installations). This requires uncertainty to be determined to within 7.5% (k=2), for activity data, and therefore 2.5% (k=2) for emissions factor. It is recognised that installations warrant review on a case-by-case basis and, in some instances, a lower-tier approach may be applied.

2.2 Observations on Uncertainty Specifications in EU ETS MRG

The MRG states that the uncertainty is on the data submitted over the reporting period. This is currently annual to EU ETS but may change in future phases of the scheme. The regulator may also require reporting at more frequent intervals. As will be discussed in this paper, the variability of the conditions in a flare line make it especially important to ensure that the calculations take into account variations in both flowrate and emissions factor. When these conditions change, the associated uncertainty changes. This makes it difficult to assess the uncertainty over any reporting period as a constant value.

The EU ETS MRG does not detail how the uncertainty of a variable emission factor should be derived and reported. In the absence of clear regulator guidance it has been decided that the most practical determination for the reportable figure is:

The flow-weighted mean of the emission factors across the reporting period

It is also noted that how the uncertainty is attributed (i.e. to activity data or emission factor) can affect whether the EU ETS uncertainty targets can be met. In reality, it is the amount of CO_2 emitted to atmosphere, and therefore the uncertainty on the reported mass of CO_2, that is important.

Under the current regime, an operator has to report activity data and emission factor. Therefore, it is possible to meet uncertainty requirements as calculated for total CO_2 but fail the target uncertainty on the precursor measurements of activity data or emission factor. An example of this is given in Appendix A.

In addition, it is not always convenient (or possible) to split the uncertainty into two parts. Any correlation needs to be considered to avoid double-accounting.

3 FLARE SYSTEMS ON THE GYDA PLATFORM

The analyses described in the following sections use terms that are described in the definitions section of this paper.

The Gyda installation has two flare systems - the high and low pressure flares designated LP and HP. These flares are continuously purged with a nominally constant flow of nitrogen (as shown in Fig. 1). Both LP and HP flare systems have GE Sensing ultrasonic flare gas meters (FGMs) installed configured to return both flowrate and the molecular weight of the *emission gas* (i.e. the total gas going to the flare).

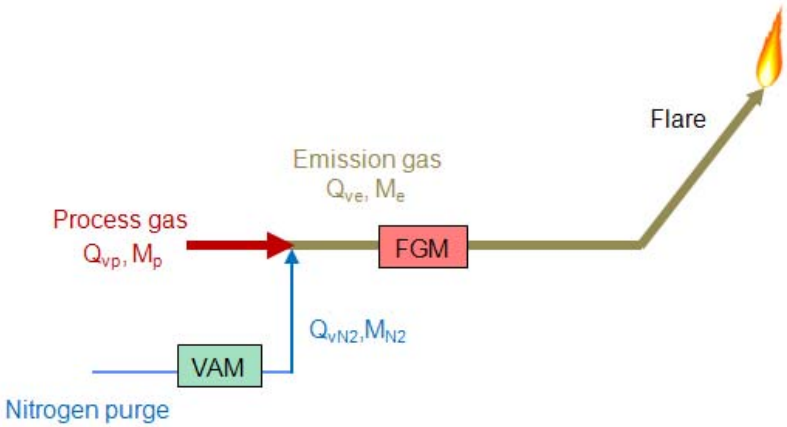

Figure 1 – Simplified diagram showing nitrogen purge and metering systems on Gyda

The nitrogen is injected upstream of the flare gas meter; therefore, the total volume of gas going to the flare tip (the *emission gas*) is a mixture of *process gas* (i.e. hydrocarbon with low levels of inherent CO_2 and nitrogen) and additional injected nitrogen.

The emission gas flowrate, Q_{ve}, can be expressed as:

$$Q_{ve} = Q_{vp} + Q_{v_{N2}}$$

Where Q_{vp} is the volume flowrate of gas generated by the process and discharged to the flare line and Q_{vN2} is the volume flowrate of the nitrogen used to purge the flare line. The gas

streams also have molecular weights associated with them (M_e, M_p and M_{N2} respectively) as depicted in Fig. 1.

Since Q_{vN2} is nominally fixed, this means that the percentage nitrogen reduces as the process gas flowrate increases. It is therefore important to take account of the effect of nitrogen on the emission factor during periods of low flaring, but less important during periods of high flaring.

The ultrasonic meters on Gyda make use of pressure and temperature measurements in internal calculations so as to calculate the output in mass units, but currently only the pressure is returned separately to the data recording system, along with the mass flow rate. Density of the emission gas is calculated from p, T and its molecular weight, M_e. M_e can be entered as a constant value or estimated from speed of sound measurements as per the proposed method detailed in this paper.

The nitrogen flow is measured by variable area flowmeters (VAMs). These measurements are then used, in conjunction with emission gas flowrate, to give values for emission factor, volumetric flowrate and, hence, the estimated mass of CO_2 being produced.

Currently, and in common with other installations, the pressure and temperature of the nitrogen at the VAM is not being measured. A VAM scale is normally configured to read in standard volume units assuming a particular gas and assumed line conditions. Any variation in the pressure and temperature about these assumed values should therefore be allowed for.

The mass flowrate of nitrogen is computed assuming an ideal gas from the volume flowrate at standard conditions.

4 CALCULATION OF THE EMISSION FACTOR WITH NITROGEN INJECTION

The amount of CO_2 emitted during combustion arises from the oxidation of carbon with the oxygen in ambient air. In addition, any CO_2 inherent in the flare gas will also pass through the flare to atmosphere. Therefore, the mass of CO_2 emitted can be calculated from the overall carbon content of the flare gas and the molecular weight of the various components.

The quantity of nitrogen in the flare gas must also be taken into account in order to calculate the correct amount of CO_2 released per unit quantity of gas burned.

One approach is to infer the nitrogen content from changes in the molecular weight of the emission gas compared with that of the process gas. Although this method has some advantages, it will be inaccurate if the molecular weight of the hydrocarbon gas is close to that of nitrogen. One way of dealing with this is to segregate the data into “purging” and “flaring” modes and then analyse the molecular weight accordingly [3].

In the current case this is done by measuring the flow rate of nitrogen in addition to the flow rate of emission gas measured by the flare gas meters.

There are two ways of calculating the amount of CO_2 released from knowledge of the flowrate of flare gas and its molecular weight:

1) Subtract the nitrogen flow from the activity data and express the emission factor as a function of carbon content of the fuel gas (tCO_2/Sm^3 of hydrocarbon gas)

2) Include the nitrogen flow in the activity data and recalculate the emission factor to effectively reduce the amount of CO_2 emitted per unit of gas flared

Method 1) Involves reducing the activity data figures that will be output from the flare gas meter and is discussed by other authors [3], whilst method 2) reduces the emission factor accordingly.

It is not clear from regulatory guidance whether activity data reported to the regulator should be the total gas measured by the metering systems or whether this can be a modified figure as is the case in method 1.

The choice of method may affect which uncertainty value is increased – activity data or emissions factor; however, provided the same methodology is applied to determine molecular weight etc. the overall uncertainty in reported mass of CO_2 emitted should be the same (as discussed previously in Section 2.1 and the example shown in Appendix A).

4.1 Calculation Procedure for Emission Factor

TUV NEL have developed a methodology that can be used be used to calculate the emission factor directly using the measured molecular weight of emissions gas, M_e, and various other inputs including flowrates. This is given in Appendix B. The methodology is based on the following underlying assumptions:

- The volume fraction of water vapour and other non-hydrocarbons (such as He, H_2S etc.) is insignificant.
- Liquid levels (e.g. water and any liquid hydrocarbons) are negligible in the flare lines
- The relative proportions of hydrocarbons, CO_2 and N_2 found in the process gas, as measured at the fuel or export gas lines, are representative of what is found in the flare line and these remain fixed across the flow range.
- It is assumed that only light, alkane hydrocarbons of the form $C_nH_{(2n+2)}$ are present in the gas (i.e. no significant amounts of aromatic compounds or alkenes are present).
- Any variation in compressibility (Z) of the mixture is negligible and an ideal gas compressibility Z=1 can be assumed. A more accurate estimate of Z could be calculated provided the gas composition can be estimated.
- Complete combustion occurs with all carbon being oxidized to form CO_2 (as implied by the oxidation factor being set to 1.0 in the MRG). Other factors may be used as appropriate.

Figure 2 is a schematic of the calculation process for determining activity data (emissions gas volume) and emission factor in terms of standard volume (m^3). The procedure is similar for parameters expressed in mass units except that there is an additional calculation for density to be included. The uncertainty will be the same in either case provided care is taken to avoid double-accounting of terms.

It is noted that the tier-level uncertainties stated in the EU ETS MRG for flares specify reporting in standard volume units

The inputs to the emission factor calculation are:

- Emissions flowrate (activity data), Q_{ve}, as measured by the ultrasonic meter
- Nitrogen flowrate, Q_{vN}, as measured by the VAM (nominally constant)
- Emissions gas molecular weight, M_e
- Process gas sample data (namely fractions of hydrocarbons, x_p, fraction of CO_2 and N_2 (y_p & z_p respectively).

Other non-hydrocarbon components can be accounted for as necessary but Talisman have advised that these are negligible in the current application.

An ultrasonic meter provides outputs of velocity of sound (m/s) and actual volume flowrate of emissions gas, Q_{ve} (m^3/s). These are the fundamental measurements related to measured transit-times and meter geometry. Measured pressure and temperature, as well as constants

such as the pressure and temperature at standard conditions (p_s, T_s) and Z/Z_s (assumed = 1.0 at low pressures found in the flare lines), allow conversion to standard volume (Sm^3) in the meter's flow computer.

The molecular weight of emissions gas, M_e, is calculated in the meter's flow computer using a proprietary algorithm which also corrects speed of sound for temperature and output to the supervisory computer. The supervisory computer records and stores this data using a proprietary data base; the OSIsoft "PI database".

In theory at least, the uncertainty in the emissions gas flowrate (i.e. activity data) will be unaffected by the addition of nitrogen. However, the molecular weight correlation will be affected to some degree by the introduction of significant amounts of inert gas which tends to move the composition away from a typical hydrocarbon gas. This was considered in the analysis.

Talisman are currently in dialogue with the meter vendor as regards ways to optimise the molecular weight correlation.

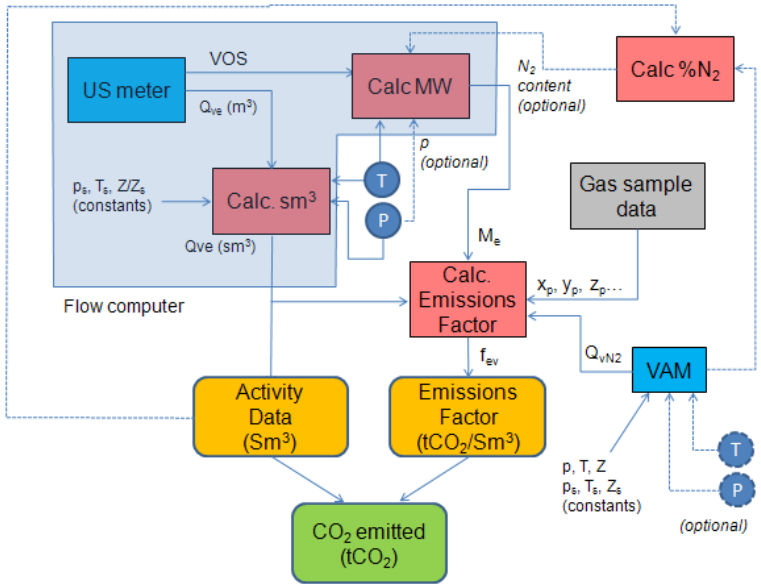

Figure 2 – Suggested calculation procedure for determining activity data and emission factor on the Gyda platform (a similar calculation is planned for other facilities)

4.2 Data Analysis

Gas flaring is not a continuous or steady-state activity; therefore, the emission factor is not a constant value. A simple arithmetic mean of emission factor over the reporting period may not be accurate because it does not take account of periods of high flow. During significant process events large volumes of gas are flared and the associated molecular weight is likely to be significantly different than that found during day-to-day flaring. Therefore, the emission factor is not a single value, but must be evaluated continuously and then used to estimate the CO_2 produced.

The flow-weighted mean and the associated uncertainty can be derived in two ways:

1) A running average of the flow-weighted mean value can be calculated across a reporting period.
2) The mean emission factor is calculated from the total standard volume of emission gas and total CO_2 generated.

The second method is the simpler of the two. The above approach required an algorithm to be programmed and TUV NEL created this using VBA coding within Excel. The VBA code analyses the raw data from an input file and can be generalised to cope with data from various flare systems. The results are output into Excel worksheets in the form of tables.

In order to determine the uncertainty, a raw data file was extracted from the PI database and the algorithm then calculated all the relevant parameters. The sheet generates values for activity data, emission factor, and quantity of CO_2 produced for each data point. It also generates, in absolute terms, the uncertainty in emission factor and CO_2 for each point. The mean emission factor uncertainty (see later discussion) and the total absolute CO_2 uncertainty are then calculated for the chosen calculation period.

The uncertainty was carried out by inserting each data point in turn into a Excel-based uncertainty budget table. The uncertainty calculations followed the methodology set out in ISO 5168 (2004) [4].

4.2.1 Process Gas Composition (Gyda)

Table 1 shows export gas sample data on Gyda over a 5-month period. It can be seen that the export gas stream is relatively stable with an average molecular weight of about 22.6 g/mol. The hydrocarbon content is about 97% by volume, the remaining 3% being made up of N_2 (0.5%) and CO_2 (2.5%). As discussed previously, this gas is viewed to be largely representative of the process gas that enters the flare line during normal operation.

Thus, in calculating the CO_2 emission factor, the inherent assumptions are made that, regardless of the source of the gas (e.g. first stage separator, suction scrubbers etc.), the N_2 and CO_2 level will be fixed, no additional inorganic gases will be present and, by inference, the hydrocarbon content of the process gas will also be fixed at around 97% by volume.

Table 1 – Gyda export gas sample data as supplied to TUV NEL by Talisman Energy

Mole Fraction					
C1	0,7217	0,7294	0,7270	0,7160	0,7180
C2	0,1391	0,1360	0,1381	0,1393	0,1381
C3	0,0714	0,0675	0,0698	0,0728	0,0716
IC4	0,0085	0,0079	0,0081	0,0088	0,0087
NC4	0,0207	0,0193	0,0197	0,0219	0,0218
IC5	0,0038	0,0036	0,0033	0,0043	0,0043
NC5	0,0036	0,0035	0,0031	0,0042	0,0043
C6	0,0024	0,0023	0,0012	0,0022	0,0026
C7+	0,0000	0,0000	0,0000	0,0000	0,0000
N2	0,0035	0,0050	0,0036	0,0041	0,0038
CO2	0,0253	0,0255	0,0261	0,0264	0,0268
TOTAL	1,0000	1,0000	1,0000	1,0000	1,0000
Physical Characteristics of C7+					
C7+ Molecular Weight	0,000	0,000	0,000	0,000	0,000
C7+ Specific Gravity	0,0000	0,0000	0,0000	0,0000	0,0000
Composition Condition					
H2S Content (mg/m3)	0,0000	0,0000	0,0000	0,0000	0,0000
Specific Gravity	0,7820	0,7741	0,7738	0,7883	0,7881
API (60F)	0,000	0,000	0,000	0,000	0,000
Molecular Weight	22,559	22,322	22,324	22,750	22,732
BS&W (Wt. Frac.)	0,000000	0,000000	0,000000	0,000000	0,000000
Salt Content (Wt. Frac.)	0,000000	0,000000	0,000000	0,000000	0,000000

4.3 Examination of Data from Gyda Flare Gas Meters

The flow and molecular weight data was analysed for the Gyda LP and HP flares over a period of 50 days (July 01 – Aug 19 2009) (as given in Table 2). These data have been derived from the flow meter data supplied to TUV NEL and were obtained from interrogation of the customer's database (the "PI database").

Flow data is taken from the actual archived flow values whilst the molecular-weight values are interpolated from the recorded molecular weight values to coincide with the same time points as the flow rate (see later description of PI data collection method).

The gas appears to be heavier and more variable on the LP flare (varying from 25.6 – 37.3 g/mol) than on the HP flare (23.5 – 32.0 g/mol). What is immediately apparent is that the molecular weight of the gas on both the LP and HP flares always exceeds the molecular weight of the export gas (22.6 g/mol).

This can be explained, in part, by the addition of the nitrogen which, at a molecular weight of 28 g/mol, will tend to increase the average molecular weight of the emission gas. However, some of the increase in molecular weight is likely due to heavier hydrocarbons entering the process gas during specific flaring events.

The data given in Table 2 appears to show that the flow rates through the Gyda LP and HP flare lines are moderately low and the risk of liquids occurring due to carry-over from the separators and/or condensation, due to temperature drops, is minimal. However, the Reynolds numbers are very low in both installations and this causes other issues for uncertainty as discussed later.

Table 2 - Summary of flow and molecular weight data for Gyda LP and HP flares based on 50-days' worth of data

	LP flare			HP flare		
	Min	**Average**	**Max**	**Min**	**Average**	**Max**
Q_{me} (kg/hr)	15.0	47.3	198.9	48.8	93.1	448.8
Q_{ve} (Sm^3/day)	294	931	5298	1057	1962	8552
M_e (g/kmol)	25.6	27.1	37.3	23.5	25.3	32.0
p (bar abs)	0.99	1.00	1.03	1.07	1.09	1.11
Re_D (approx)	3303	10,421	43,803	2634	5028	24,250
Velocity (m/s)	0.2	0.65	3.7	0.04	0.08	0.33
N_2 content (%)	2.0	11.6	36.7	5.6	24.5	45.4

Notes:
[1] The values for max/min values for N_2 content and M_e do not necessarily correspond to max/min flow rate values
[2] Pipe Reynolds number, Re_D, based on assumed viscosity for methane of 1.1 x 10^{-5} kg/m-s
[3] Velocity based on average pressure & ambient temperature

It should be noted that the above observations are based on a limited set of data spanning only 50-days and it is recognised that more variable conditions may occur on occasion during a given year. In addition, changes to the facility (e.g. tie-backs to subsea platforms, system upgrades etc.) in subsequent years may also change the flow rates, line conditions and gas composition. There may be a requirement to revisit the uncertainty analysis in such cases.

5 FLOW MEASUREMENT

As previously discussed the flow rate of the total gas flared (the emission gas) and the nitrogen injected is needed to determine the emission factor. These measurements are discussed in more detail below.

5.1 Emission Gas Flow Rate

The emission gas flow rate is measured using single-path flare gas ultrasonic meters. The flare gas meters installed on Gyda are single-path transit time ultrasonic meters with the beams at an angle of 45° to the flow. The primary measurement is the transit time difference, Δt, which varies as a function of the velocity.

The volume flowrate is calculated within the meter from knowledge the pipe diameter, an assumption of an 'ideal' flow profile, and the measured velocity along the path.

Volume flowrate can be calculated at standard reference conditions using the following equation

$$Q_{ve} = kA\left(\frac{L}{2\cos\theta}\frac{\Delta t}{t_{21}t_{12}}\right)\left(\frac{p_s}{p}\times\frac{T}{T_s}\times\frac{Z}{Z_s}\right) \text{ (Sm}^3\text{/s)} \quad (1)$$

From an uncertainty point of view, the key input parameters in the above equation are the transit times, t_{12} *and* t_{21}, correction factor, k, and pipe area, A. The path length, L, and beam angle, θ, should be known to a reasonable accuracy.

Velocity of sound, c, can also be determined from the transit times and path length, L, using

$$c = \frac{L}{2}\left(\frac{t_{21}+t_{12}}{t_{21}t_{12}}\right) \quad (2)$$

The molecular weight is calculated from c using a proprietary algorithm which was supplied to TUV NEL for analysis. The algorithm calculates the molecular weight of emission gas, M_e, from c and measured temperature assuming that the gas is mostly made up of hydrocarbons.

There is currently no facility for correcting molecular weight for significant nitrogen content or increased gas pressure. However, recent advances to the technology allow these corrections to be made so there is the option to upgrade the meters in the future.

For this application, the meters used are configured to measure and return the mass flowrate. Since the calculation of mass is an intermediate step in determining mass of CO_2 emissions, the uncertainty analysis is effectively carried out on the fundamental measurements of standard volume.

5.2 Nitrogen Purge Meters

The flow of nitrogen is reportedly maintained at a constant rate and measured using on-line variable area flowmeters (VAMs). The nitrogen flowrate is read and recorded manually once a day for quality control and monitoring purposes and to ensure the flare remains safely purged.

This is a typical installation in the North Sea sector where low accuracy meters, originally installed for process control, are now being used as part of the measurement system. There was no indication of the standard conditions which have been assumed when setting the VAM flow scale (range). It was assumed that 'normal' conditions of 0°C and 1.01325 bar were specified, however it is known that the manufacturer of these particular meters normally use 15°C or 20°C. In common with many purge gas meters, the calibration and traceability of these VAMs was not as strictly controlled as might be expected for a regulated system.

As no measurements of pressure and temperature were taken at the VAM it was assumed that the meter operates marginally above the flare gas pressure (approximately atmospheric pressure) and is assumed to operate at ambient temperature.

No correction for errors due to incorrect standard conditions is being applied.

5.3 Data Logging and Reduction

Before embarking on an uncertainty analysis it is important to appreciate the method of data logging and reduction. This requires a comprehensive understanding of the measurement process from the instrumentation, data acquisition and any subsequent calculations, through to the PI database.

The measurements associated with the measurement of the emission gas are pressure, temperature, flowrate and molecular weight. Typically, pressure is measured well upstream of the meter (in the current case at the knock-out drum) and is read by the ultrasonic meter's flow computer and returned to the supervisory computer (in this case a Honeywell DCS system).

Flowrate and molecular weight are calculated by the meter's flow computer and also returned to the DCS. Temperature is measured by a probe located downstream of the ultrasonic meter and read by the meter flow computer. This is not currently being returned to the DCS (all calculations being carried out within the flow computer).

The DCS interrogates the meter at a given sample rate (believed to be 15 seconds). The DCS returns these values to the PI database for archiving. The PI interface software then carries out 'exception filtering' allowing only measured data points which change significantly from the previous reading to be sent to the main PI server application. This reduces the amount of data sent to the main PI database server.

Data sent to the PI database server is subject to further 'data compression' whereby data not following a specific linear trend is excluded, once again allowing a reduction in data archived, without any (apparent) loss of significant information. All stored points are archived with a date and time-stamp.

5.3.1 Examination of the Recorded Mass Flow Rate from the Gyda LP Flare

Archive data can be retrieved in different ways from the database and this will have been archived from raw data with different degrees of filtering and analyses. It is noted, however, that only the archived data, after exception and compression filtering, can be retrieved.

The first retrieval method used was to request data at specific time intervals. This is the method employed in previous analyses and was initially proposed to be used in this work.

Data at five-minute intervals was proposed to best follow the perceived frequency and magnitude of the flare flowrate variations. This information was generated based on a linear interpolation between the archived data before and after each selected time value.

Figure 3 shows the emission gas flow rate, and corresponding molecular weight, during a flare event occurring in the LP line. If data is collected from the archive at 5-minute intervals, then it can be seen that the high flare event is not adequately resolved.

The second retrieval method is to return each archived flowrate value. It is noted that these are not regular intervals owing to the data compression being applied; however each value carries an accompanying time stamp or tag. Similar data for molecular weight is available but the data points would be asynchronous with the flow data.

For this examination, molecular weight data was returned as interpolated data at the same tag times as the flow data. It would be difficult to obtain molecular weight data coincident with each flowrate in any other way unless the sequence of data logging was changed and flow and molecular weight data were recorded together.

The archived data appears to follow what would be expected from an event. It is noted that molecular weight variation follows the flow event – in this case it reduces as the flow increases (and the percentage of nitrogen reduces). This reflects the situation where the hydrocarbon content is significantly above that of the export gas, but the percentage of the nitrogen has reduced. As molecular weight at this time is based on interpolated values taken between successive flowrates, some damping of the variation is observed.

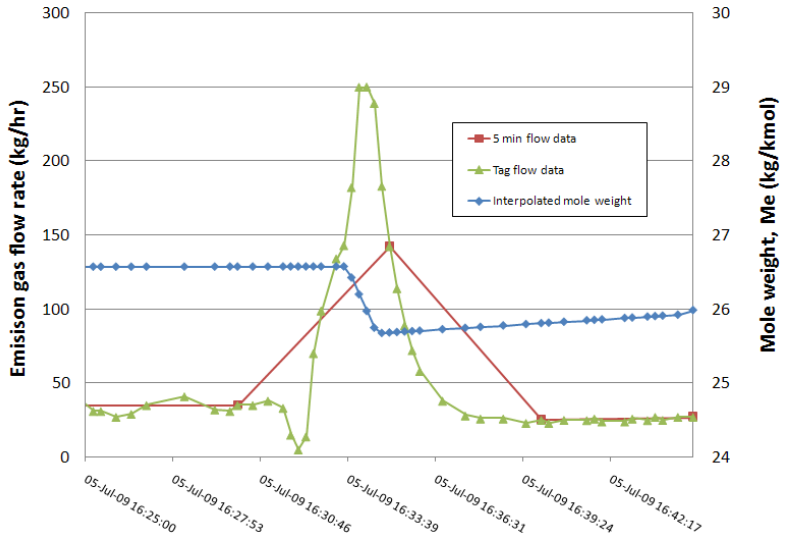

Figure 3 - Flowrate and Corresponding Molecular Weight Data Obtained from the PI Database During a Specific Flaring Event (Gyda LP Flare)

For the purpose of determining uncertainty, no further investigation of the effect of data recording was thought necessary; however, it is recommended that a more detailed investigation should be carried out to determine the best data recording methodology in the future.

6 MEASUREMENTS AND UNCERTAINTY SOURCES

The overall uncertainty in emission factor was calculated using the Excel spreadsheet and accompanying VBA code. The equations in Appendix B were effectively differentiated to produce the sensitivity coefficients and the individual uncertainties were combined to produce the overall uncertainty for the emission factor.

Although TUV NEL were not specifically asked to look at the uncertainty in activity data (emissions gas flowrate) this was a necessary input to the calculation of nitrogen volume fraction and therefore had to be considered in calculating the emission factor.

6.1 Treatment of Type A and Type B Uncertainty Components

The algorithm calculates uncertainties for each individual data point. However, it is recognised that a significant proportion of the uncertainty is a type B (systematic component), whilst the remainder is a type A (random component). To calculate the uncertainties for the reporting period, and hence the uncertainty of the mean emission factor, separation of the type A (random) and type B (systematic) contributions has to be carried out, evaluated and then combined separately.

The type A uncertainty can be evaluated using statistical techniques based on the calculation of standard deviation of the data. Alternatively, where appropriate, the uncertainty of the mean is the uncertainty of a single point divided by the square root of the number of degrees of freedom of the data set. The latter approach has been adopted for this study. Type B (systematic) uncertainties were combined by using the approach set out in ISO 5168 [4].

The type A and type B uncertainties were finally combined by root-sum-square addition. It is considered that type B uncertainties will be dominant. In analysing the uncertainty contributions, it is clear that most of these will have components which are both type A and type B. In the analyses, each contributor was allocated a proportion of its uncertainty to type A and type B based on a judgement of the uncertainty source. Although somewhat arbitrary, if in future the allocation requires to be adjusted to include output from more rigorous analyses, this can be easily incorporated in the uncertainty model.

An overview of the uncertainty calculation and the assumed values for a single data point are given in Table 3.

Table 3 – Uncertainty Sources for a Single Data Point

Uncertainty in Emission gas MW						
Nitrogen fraction	0.1522					Basic speed of sound equation. MW = antilog(7.012 – 1.836 * log10 c_ref)
Source	Unit	Value	U	U*	% type B	
Mol weight measurement	g/mol	27.29	0.819	**3**	100	U based on manufacturer's estimates
Pressure	Pa	100619	503.1	**0.5**	75	Pressure has an insignificant effect
Temperature	K	288.15	**1**		75	Temperature also has an insignificant effect
additional due to High N	g/mol	27.29	0.042	**0.1522**	100	Incorrect correlation due to high N2. U assumes correction is made.
PI						Possible U for data logging set to zero at the moment.
Mol weight		27.29	0.946	3.4686	**100.00**	

Uncertainty in Emission factor for period based on NEL method						
Source	Unit	Value	U	U*	% type B	
Emission gas flow	Sm3/hr	28.879927	**1.447**	**5.0109**	78.94	Uncertainty from above
Nitrogen flow	Sm3/hr	4.3958775	**0.565**	12.843	45.95	Uncertainty from above
Mol weight E gas	g/mol	27.29	0.95	3.47	100.00	Uncertainty from above
Fract CO2 in gas	%	2.53	0.1	3.9526	50	Estimate of uncertainty in determining CO2 inherent
Fract Inerts in gas	%	0.35	0.04	11.429	50	Estimate of uncertainty in determining N2 inherent
Emmission factor	kg/Sm3	2.889	0.152	5.2559	**75.13**	

Uncertainty in CO2						
Source	Unit	Value	U	U*	% type B	
Emmission factor	kg/Sm3	2.889	0.152	**5.256**	75.13	Based on above
Flow e gas	Sm3/hr	28.880	1.447	**5.011**	78.94	Based on above.
CO2 rate	kg/hr	83.421	6.058	7.2618	**76.87**	

6.2 Bias Errors

In the uncertainty analysis any error due to incorrect application of the variable area meter (VAM) corrections is not considered. Similarly, the error in molecular weight due to nitrogen content has been assumed to have been corrected for. These are examples where bias errors have been introduced and should be corrected for rather than being included in the uncertainty.

If bias errors cannot be corrected for they should be included in the uncertainty statement; in such cases an asymmetric uncertainty band must be calculated (e.g. x ± y where x is the systematic bias (error) and y is the uncertainty about this bias).

6.3 Main Uncertainty Sources

With reference to the equations in Appendix B, and assuming constants to be correct and to an adequate number of decimal places, the main sources of uncertainty are:

1. Volume fractions of components in process gas, x_p, y_p, z_p
2. Flowrate of nitrogen gas, Q_{vN2}
3. Flowrate of emissions gas, Q_{ve}
4. Emissions gas molecular weight, M_e

These key sources are discussed in more detail below.

6.3.1 Process Gas Composition

The process gas is the gas that enters the flare line from the various sources (such as first stage separator, gas scrubbers vessels etc.) prior to nitrogen injection. The relative fractions of hydrocarbon gas (alkanes), CO_2 and nitrogen is assumed to be the same as for the export gas for both the LP and HP flares (i.e. the volume fractions – as derived from Table 1 - are as follows):

Hydrocarbon fraction, x_p = 97%
CO_2 fraction, y_p = 2.5%
N_2 fraction, z_p = 0.5%.

The uncertainty of this assumption must include any estimated differences in the composition of the process gas from that of the export gas.

If a process upset occurs, the flowrate of gas increases markedly and the composition of the gas changes, depending on the nature of the event.

The uncertainty in the CO_2 and N_2 fractions (expressed as a percentage) are taken to be 0.04 and 0.1% respectively. The hydrocarbon content is simply determined as $x_p = 1 – (y_p + z_p)$ and its uncertainty is subsumed in the calculation of M_e.

Note: The uncertainty in compressibility is assumed to be negligible as the line pressure and temperature will be close to ambient the majority of the time.

6.3.2 Uncertainty in the Nitrogen Flowrate, Q_{vN2} (as measured by a variable area meter)

The nitrogen flowmeters are variable area meters set up to indicate in standard volume units (Sm^3/hr). These devices have a stated uncertainty of 2% of span. The LP meter has span of 25 Sm^3/hr while HP meter has span of 100 Sm^3/hr. The set flowrate was 4.5 Sm^3/hr for the LP meter and 20 Sm^3/hr for the HP meter. Therefore 2% of span equates to an uncertainty of reading of 11% for the LP meter and 10% for the HP meter respectively.

In the absence of any significant meter data, the set value is taken to be nominally constant. Therefore, the consistency of the manual reading and setting, any effect of changes in nitrogen supply and pressure and temperature, can only be speculative.

Pressure, temperature and barometric pressure are not currently recorded. Correction is not applied for actual density of the nitrogen and, in fact, some doubt remained as to the actual meter conditions. The lack of correction is considered to generate an error. The magnitude of the error has been assessed, however only the uncertainty in the error has been included in the budget. However these errors were included within a list of bias errors.

It would be advisable to measure temperature and pressure at the nitrogen meters (even at a relatively low accuracy), and to correct the readings in order to reduce uncertainty and remove a potential source of bias.

6.3.3 Uncertainty in the Emission Gas Flowrate, Q_{ve} (as measured by flare gas ultrasonic meter)

Detailed uncertainty analyses of the performance of ultrasonic meters had been carried out previously [5] and from this, and the manufacturers estimate of uncertainty, an uncertainty of 4% was assumed as a baseline value for the Gyda flare gas meters. Additional uncertainty needs to be included to account for deviations from ideal, fully developed flow conditions.

The meter vendor quotes an uncertainty of between 2.5% to 5% between the limits 0.3 m/s to 100 m/s. Uncertainty will increase at velocities below 0.3 m/s and this is an area where the meters are operating.

Although the meter is specified to work between 0.03 – 0.3 m/s, the uncertainty will be a lot higher because the timing resolution starts to dominate. To cover this, each meter was allocated a “low-flow cut-off point” below which the uncertainty starts to rapidly increase.

An additional increase in uncertainty is encountered if the Reynolds numbers are such that the flow regime becomes laminar/transitional. This is due to incorrect flow profile corrections. Bias errors will be evident in such cases; however, these are difficult to quantify in the transition region.

Currently the uncertainty analysis assumes that this error will be within the increased uncertainty already included at low-velocity. This may require more detailed examination if uncertainty is to be more accurately determined.

Additional uncertainty will be introduced if an "non-ideal" flow profile is evident across the measurement plane. An uncertainty due to installation effect has to be recognised; however, this is difficult to assess without detailed drawings of the installation. CFD simulations of the installation can be carried out determine the installation error [6].

Some additional uncertainty was included to take account of pipe roughness at high Reynolds numbers which will affect the flow profile and, therefore, the meter factor.

Temperature and pressure uncertainties also are included in the uncertainty budget. As absolute transducers are used for pressure, no uncertainty needs to be considered for variations in barometric pressure. Although pressure is measured at the knock-out drum upstream of the meter it is assumed there is no pressure loss between the drum and the meter. It is not currently known where the temperature is measured but it is assumed to be close to or near the meter.

A nominal value has been included to cover installation (non-ideal flow profile) effects and pipe diameter variation has been included but may require modification following a full assessment of the metering installation.

6.3.4 Uncertainty in Molecular Weight Correlation, M_e

The molecular weight correlation is known to be affected by the volume fraction of inert and non-hydrocarbon (inorganic) gases, such as nitrogen, water vapour, hydrogen etc. The presence of these gases will cause the calculated molecular weight to be in error. In addition, the presence of liquids will cause serious problems with the molecular weight correlation (and also the measured flow rate).

It is currently assumed that the meter algorithm is configured to assume a typical hydrocarbon gas and has not been adjusted to recognise the high nitrogen concentration, nor the variability of this concentration with flowrate. If the nitrogen concentration is not accounted for, a significant error in the molecular weight (and indeed the mass flowrate) will be evident.

A proprietary algorithm is used to correlate the measurement of speed of sound and local temperature. The algorithm is based on an empirical fit to various hydrocarbon gas mixtures.

The overall uncertainty in M_e owing to timing resolution, path length, temperature correction and curve-fit to the gas data is stated as 3% in the uncertainty reports (for activity data in mass units) supplied to TUV NEL from Talisman [5]. In addition to this there will be uncertainty in M_e due to pressure and the presence of non-hydrocarbons.

The main issue for the molecular weight correlation is the injected nitrogen which is not currently being accounted for.

<u>Effect of Nitrogen on the Molecular Weight Correlation</u>

The error in the molecular weight correlation was assessed by calculating speed of sound for a range of gas mixtures using the AGA 10 method. This sound speed was then input to the equations at 0°C, 20°C and 30°C and the calculated value of M_e was compared with the actual molecular weight of the gas mixture.

The percentage error (referred to the case where no nitrogen is injected into the flare line) was seen to be linear with nitrogen content. Thus, at 50% N_2, the error is -5.2% and it is -2.6% at 25% N_2. Discussions with the meter vendor reveal this to be a realistic number, comparing well with their own analyses with methane/N_2 mixtures which showed a -5.8% difference between 50% and 0% N_2 (i.e. 100% methane) [7].

As part of the calculation process, both the flowrate of nitrogen and the total flowrate of emission gas are measured. It would be possible, therefore, to correct the molecular weight reading for the added nitrogen. This correction could be incorporated into the flowmeter software provided the nitrogen flowrate remains constant or can be dynamically read by the meter.

In the uncertainty analyses it was assumed that the molecular weight will be corrected - either online (e.g. through input of the nitrogen fraction into the meter via a 4-20 mA signal) - or offline in the PI database. These options are currently being looked into.

Effect of Pressure on Molecular Weight Correlation (Gyda)

It can be shown that the sensitivity of M_e to temperature is small (in any case, it is included in the aforementioned uncertainty analyses). However, the correlation does not currently take account of the effect of pressure on M_e.

The effect of pressure on M_e was determined for pure methane using TUV NEL's Physical Properties Database Software (PPDS) which showed this to be < 0.23% per bar over the range 1 – 10 bar for temperatures of 0 - 30 °C. Since the data supplied by Talisman shows that the line pressure is close to atmospheric almost 100% of the time this uncertainty source has been effectively ignored.

7 RESULTS OF THE UNCERTAINTY ANALYSES

Data was provided from Gyda for the period July-August 2009. For the LP flare this consisted of some 108,000 data points which were provided as two separate data files. The HP flare had some 60,000 data points and these were provided as one data file. These files were analysed using the customised spreadsheet.

Periods where a measurement was clearly in error (e.g. low or high flowrates), impossible molecular weights etc., were identified and given an agreed default value and uncertainty. It was noted that the time intervals between some data points were unusually long. It could be that the flowrate was very stable or it may indicate that something had happened to interrupt the readings without obvious discrepancy on the data at the start or finish of the interval. No attempt was made to investigate these instances further and it was therefore assumed that the flowrate was stable during these periods.

The results of the analyses of the three Gyda data sets are given in Table 4. The LP flare data was analysed in two sets to reduce run time. The algorithm could be optimised to cope with larger data sets; however, for future emissions calculations it would make sense to calculate the uncertainty in the data as it is logged - either for each point or on an hourly basis etc. - and then store these figures into the PI database. An added advantage is that the uncertainty can be tracked in a more timely fashion.

Table 4 – Summary of uncertainties for the Gyda flare lines

Flare line	Start date	Finish date	F-W Emission factor (kg/Sm^3)	Mass of CO_2 emitted (tonnes)	Uncertainty in mean Emission factor (%)	Uncertainty in mass flowrate (%)	Overall Uncertainty[1] in mass of CO_2 (%)
HP	1 July	19 Aug	2.9	217.7	4.1	6.8	7.9
LP set 1	1 July	30 July	3.0	79.5	4.4	3.3	5.5
LP set 2	1 Aug	19 Aug	3.1	57.4	4.8	2.9	5.6

[1] Note: These uncertainties can be viewed against a calculated overall uncertainty limit for mass of CO_2 which is 7.9% (k=2) for tier 3.

The estimated uncertainty on mean emission factor varied between 4.1% and 4.8% with a coverage factor of k=2 (approximating to 95% confidence interval). The uncertainty figures are similar for the HP and LP flares.

Although this uncertainty is higher than the tier 3 limit of 2.5%, it is noted that the overall uncertainty on mass of CO_2 is between 5.5% and 7.9% and therefore falls within the overall uncertainty limit on CO_2 (7.9%) as calculated from the tier 3 limits for activity data and emission factor.

Once again, it is noted that the above results are based on 50-day's worth of data which may not be enough to completely define the limits on the process conditions.

8 CONCLUSIONS AND RECOMMENDATIONS

The uncertainty on the Gyda and Varg flare systems was assessed for Talisman Energy Norge AS [8]. This paper concentrates on the results from the Gyda flares. A significant part of this work was in producing a revised calculation procedure for emission factor. Logging and data handling were looked into in detail and, based on these findings, a more appropriate methodology for extracting the data was suggested.

The analysis highlighted the importance of calculating the mean, flow-weighted emission factor from the raw data rather than a constant value. Since conditions can vary widely in a flare line, the importance of analysing the emissions factor based on all the available data is clear.

The analysis and archiving of the data should reflect the need to have coincident values of flowrate, molecular weight and properties. It may be advisable to have the calculation of uncertainty carried out at the data collection stage allowing a cumulative uncertainty to be generated for any time period, thus doing away with the need for retrospective analyses

The measurements of the flowrate of nitrogen need to be examined in detail. The effect of not correcting for pressure at the variable area meter has the potential for producing a very large error depending on line pressure. It would be prudent to replace the current flowmeters with more modern and accurate technology.

The effect of ignoring the nitrogen content of the gas on molecular weight will be an error of about 3 - 4% at low flare flowrates. This can be corrected offline if it cannot be incorporated in the meter in some way (e.g. live feedback of nitrogen content to flow computer).

The effect of not measuring or accurately accounting for temperature and pressure of the nitrogen is relatively small, of the order of 0.5%.

Although the calculated uncertainty in the emission factor lies outside the EU ETS tier 3 limits for the LP and HP flares, the overall uncertainty on mass of CO_2 is within the limits if the values for activity data and emission factor are duly combined. However, it is noted that these figures are based on limited data. The calculation would need to be carried out for the agreed EU ETS reporting period.

At time of writing Talisman are currently in discussion with the regulator as to whether the methodology of calculating emission factor using speed of sound output from the flare gas meter will be accepted.

9 DEFINITIONS

The following definitions have been used to describe the various parameters in the calculation process for emission factor:

Activity data: the quantity of gas flared (this redefined here as the quantity of **Emissions Gas** as below)

Emission Factor: factor relating the quantity of CO_2 produced from the emission gas after combustion to the total quantity of emission gas produced. Although emission factor may be

expressed in relative to mass or volume of emission gas, under EU ETS guidelines this is expressed as the mass of CO_2 for each Standard cubic meter of emission gas. (kg of CO_2/Sm^3)

Emissions Gas: the gas discharged to the flare. This is the **Process gas** combined with the nitrogen purge gas.

Hydrocarbon Gas: the mixed hydrocarbon gas components within the **Process Gas**.

Process Gas: The gas generated by the process and discharged to the flare line. This excludes any measured purge gas.

Standard Volume: the volume occupied by a quantity of gas if it was at defined conditions. The Standard conditions for this application are 273.15 K (0 °C) and 101325 Pa.

Normal Volume: an alternative to Standard volume conventionally applied to the conditions specified above. This is the term used in the EU ETS guidelines and as stated above.

10 ACKNOWLEDGEMENTS

TUV NEL wishes to thank Pål Jaghø, Vidar Gabrielsen and Alice Baker at Talisman Energy Norge AS for their support during the project, and Jed Matson at GE Sensing for his advice on the molecular weight correlation.

11 REFERENCES

[1] Directive 2003/87/EC of the European Parliament and of the Council of 13 October 2003 establishing a scheme for greenhouse gas emission allowance trading within the Community and amending Council Directive 96/61/EC

[2] 2007/589/EC: Commission Decision of 18 July 2007 Establishing Guidelines for the Monitoring and Reporting of Greenhouse Gas Emissions Pursuant to Directive 2003/87/EC of the European Parliament and of the Council (notified under document number C(2007) 3416) (Text with EEA relevance)
http://eur-lex.europa.eu/LexUriServ/LexUriServ.do?uri=CELEX:32007D0589:en:NOT

[3] Frøysa, K-E *et al*, Nitrogen subtraction on reported CO_2 emissions using ultrasonic flare gas meters, In 27th International North Sea Flow Measurement Workshop, 20 - 23 October, Tonsberg, Norway, 2009

[4] International Standards Organisation ISO 5168:2005, Measurement of fluid flow – procedures for the evaluation of uncertainties

[5] Usikkerhets analyse for USM flare/vent gas flowmeters: PEM-3431-UNCERT-HP-GYDA and PE M-3431-UNCERT-LP-GYDA.

[6] Gibson, J. Validation of the CFD method for determining the measurement error in Flare Gas Ultrasonic meter installations, In 27th International North Sea Flow Measurement Workshop, 20 - 23 October, Tonsberg, Norway, 2009

[7] Private Communication - Jed Matson, GE Sensing, Billerica, MA, Sept 2009.

[8] TUV NEL Report No. 2009/240 for Talisman Energy Norge AS, Evaluation of Uncertainty in Emission Factor for Gyda and Varg Oil and Gas Facilities, September 2009 (Commercially Restricted)

APPENDIX A - SAMPLE CALCULATION OF UNCERTAINTY ON TOTAL CO_2

Assuming activity data and emission factor uncertainties to be uncorrelated, the limit on overall expanded (k=2) uncertainty in CO_2 can be calculated from the limits given in the EU ETS MRG [2] for the highest tier approach (i.e. 7.5% on activity data (flow) and 2.5% on emission factor) as

$$U_{CO_2} = \sqrt{7.5^2 + 2.5^2} = 7.9\%$$

Hence, 7.9% (k=2) represents the highest uncertainty on the reported mass of CO_2 that can be tolerated.

Two possible scenarios are shown in the example below.

Operator A's uncertainty values for activity data and emission factor happen to equate to the tier 3 limits and has, therefore, only just complied with the MRG on both counts.

Operator B has failed to meet the minimum uncertainty requirement for the emission factor of 2.5%. This is despite the overall uncertainty in mass of CO_2 being 1.5% lower than Operator A's who has met the individual requirements. Obviously if the uncertainty on activity data is already close to the 7.5% limit then operator B would fail both the individual requirement on emission factor and would exceed the 7.9% uncertainty value for overall CO_2 emission.

In this case an uncertainty of up to 6.8% on activity data can be tolerated before Operator B will exceed 7.9% (as shown by the values in brackets).

Operator A

Uncertainty on activity data	= 7.5%
Uncertainty on emission factor	= 2.5%
Total uncertainty on tCO_2	= 7.9%

Operator B

Uncertainty on activity data	= 5.0% (6.8%)
Uncertainty on emission factor	= 4.0% (4.0%)
Total uncertainty on tCO_2	= 6.4% (7.9%)

APPENDIX B – TUV NEL CALCULATION PROCEDURE FOR CO_2 EMISSION FACTOR

The emission factor is simply given as the number of moles (volume) of CO_2 emitted per molar volume of gas at standard conditions; thus

$$f_{e,v} = \frac{(nx + y) M_{CO_2}}{v_{mol}} \qquad \text{(B.1)}$$

where: $f_{e,v}$ is the volume-based emission factor (tCO_2/Sm^3).
- n is the number of moles of carbon in the hydrocarbon gas
- x is the volume (mol) fraction of hydrocarbon gas in the *emissions gas*
- y is the volume (mol) fraction of inherent CO_2 in the *emissions gas*
- v_{mol} is the volume occupied by one standard volume of gas (0.022414 (Sm^3/mol at standard conditions of 273.15 K and 1.01325 bar abs).
- M_{CO2} is the molecular weight of CO_2 (g/mol).

For an alkane gas mixture it can be shown that a unique relationship exists between n and M_e regardless of the relative percentages of hydrocarbons in the mixture provided the volume fractions of hydrocarbons, CO_2 and N_2 in the process gas can be estimated and the flow of injected N_2 is known.

$$f_{e,v} = \frac{1}{v_{mol}} \left[\left(\frac{M_e - yM_{CO_2} - zM_{N_2} - 2M_H x}{M_C + 2M_H} \right) + y \right] M_{CO_2} \qquad \text{(B.2)}$$

where M_C, M_H, M_{CO2} *and* M_{N2} are the molecular weights (g/mol) of the respective components available from standard texts and z is the volume (mol) fraction of nitrogen in the emissions gas.

Equation B.2 can also be expressed in mass units; however care should be taken when analysing uncertainty components to avoid double-accounting for parameters which cancel-out on multiplication. Other non-carbon contributing components can be easily included into Equation B.2 if required.

In the absence of gas sample data from the flare line itself, the percentage of N_2, CO_2 and hydrocarbons in the emissions gas must be inferred from the fuel gas samples.

The total nitrogen fraction in the emission gas, z, is given by

$$z = \frac{Q_{vN}}{Q_{ve}} + z_p \frac{Q_{vp}}{Q_{ve}} \qquad \text{(B.3)}$$

where z_p is the volume fraction of nitrogen in the process gas

The variable y is volume fraction of inherent CO_2 in the process gas as a fraction of the emission gas. This is calculated from the CO_2 fraction in the process gas, y_p

$$y = y_p \frac{Q_{vp}}{Q_{ve}} \qquad \text{(B.4)}$$

Finally the hydrocarbon content of the emissions gas, x, can be simply calculated using

$$x=1-(y+z) \qquad \text{(B.5)}$$

North Sea FLOW Measurement Workshop

Paper 3.3

A Cost-Effective Approach on CO_2 Emission Factor Estimation For Flare Ultrasonic Metering Systems

Kjell-Eivind Frøysa
Christian Michelsen Research AS

Anders Hallanger
Christian Michelsen Research AS

Endre Jacobsen
Statoil ASA

Anders Løvoll Johansen
Statoil ASA

TÜV SÜD

nel technology for life

28th International North Sea Flow Measurement Workshop
26th – 29th October 2010

A Cost-Effective Approach on CO_2 Emission Factor Estimation For Flare Ultrasonic Metering Systems

Kjell-Eivind Frøysa, Christian Michelsen Research AS
Anders Hallanger, Christian Michelsen Research AS
Endre Jacobsen, Statoil ASA
Anders Løvoll Johansen, Statoil ASA

1 INTRODUCTION

In flare gas systems, flow measurement is important both for reports of gas emissions and for process control. Due to the nature of such systems, the flow rates in a flare line varies from very low at normal operations to full flare with very high flow rate in the case of flaring events. This means that a flow metering system for flares typically has to be able to measure flow velocities from 0.1 m/s or less, to more than 100 m/s in order to cover all cases.

The measurement of the amount of flare gas is usually carried out by an ultrasonic flare gas meter. Such meters have been in operation for several decades. They are primarily volumetric flow meters measuring the actual (line) volume flow rate of the flare gas. By calculations using the measured pressure and temperature, the volume at a selected reference condition (in Norway typically standard condition of 1.01325 bar and 15 °C) is found. Then accumulation of standard volume is carried out.

The ultrasonic flare gas meters also measure the velocity of sound in the flare gas. From the velocity of sound, pressure and temperature, the density of the flare gas can be estimated by vendor-specific algorithms. Thus, the ultrasonic flare gas meters can also provide the mass flow rate and the accumulated mass of flare gas flowing through the meter.

In the recent years, new attention has been paid to the flaring systems, due to new European regulations related to climate gas emissions [1]. For a complex system as a flare gas line, such new regulations have been challenging. The regulations have imposed new types of reports, and have to some extent suggested measurements that are at the frontier of industrial development, if not ahead. In particular this is the case for the CO_2 emission factor that is required in the new regulations. This quality factor for the flare gas has not been in focus in earlier regulations.

Such regulations have forced the industry to review their measurement systems, and evaluate how more information can be found from already existing metering stations. This is needed both in order to derive information that today is not easily measured, and in order to reduce the cost and complexity of installing new and upgraded metering stations.

In the present paper, a new and more cost-effective approach on CO_2 emission factor estimation for flare ultrasonic metering systems is presented. The approach is based on measurements already present in the flare gas metering station, in addition to some general process information for the installation in question.

In Section 2, the relevant authority requirements are presented. Thereafter, the status for flare gas metering is discussed in Section 3. This also includes possible methods for estimation of the flare gas CO_2 emission factor. In Section 4, the new method for cost-effective estimation of the CO_2 emission factor is presented. In Section 5, the uncertainty of the method is discussed, before some industrial experiences are discussed in Section 6. The conclusions are given in Section 7.

2 AUTHORITY REQUIREMENTS

The authority requirements related to climate gas emissions are focused on the two parameters (i) activity data and (ii) CO_2 emission factor.

The activity data is the annual accumulated amount of flare gas that is burnt. This can be reported either in mass or in standard volume. The expanded relative uncertainty with 95 % confidence level of the activity data shall also be documented. For large platforms, this uncertainty should be less than 7.5 %.

The CO_2 emission factor is the amount of CO_2 (mass) that is released when burning one unit of flare gas. The unit can be either a mass unit (kg) or a volume unit (Sm^3). Thus the unit of the CO_2 emission factor is either kg/kg or kg/Sm^3. Both the annual flow weighted average CO_2 emission factor, and the relative expanded uncertainty with 95 % confidence level should be reported.

3 STATUS FOR FLARE GAS METERING

In this chapter, the industrial status for estimation of activity data and CO_2 emission factor is presented.

3.1 Flow metering (activity data)

The activity data are measured by means of an ultrasonic flare gas flow meter. As discussed in the introduction, this is a volumetric flow meter. However, through the velocity of sound, such meters calculate the density and the molar mass of the flare gas. Thus, both the standard volume of flare gas and the mass of flare gas can be accumulated using such a meter. At some installations, the activity data is reported as standard volume, and at other installations activity data is reported as mass. In Norway, traditionally offshore installations have reported standard volume, and land based installations have reported mass. There is today a trend also offshore to change from standard volume to mass. This is due to uncertainty requirements on the CO_2 emission factor, and will be briefly discussed below.

3.2 CO_2 emission factor

The determination of the CO_2 emission factor for a flaring system has been a challenging task. As a starting value, a worst case factor has been used several places. This has often been selected so large that the CO_2 emission has been over-estimated. Such a factor can for example be 3.75 kg/Sm^3, close to that of ethane

A more precise CO_2 emission factor can be found by using a company specific factor. This can be based on e.g. process simulations and thus some expectations of the gas composition in the flare in question. Thus the company specific factor in many cases is more precisely called an installation specific factor.

In order to specify the CO_2 emission factor more precisely, measurements are needed. There have been several discussions related to gas composition measurements, either in form of laboratory analysis of samples of the flare gas, or by on-line gas chromatographs an the flaring line. There are, however, in general several problems with such solutions.

A gas sample can typically be taken once a week, or maybe once a day. Such a procedure is demanding with respect to man hours, laboratory use and also contains some HSE issues. Despite this, in installations where the flaring is quite constant over time, such a regime may trace the gas quality and thus the CO_2 emission factor properly, to a relative expanded uncertainty of 2.5 % with 95 % confidence level. However, in most flare gas lines, the flaring is not constant. Most of the time, there is a low flow rate, with a molar mass of the flare gas corresponding to the relevant low-flow sources, which may be continuous or of long duration. The high flaring events are shorter in duration, maybe just some minutes. However, the accumulated flow in these case may be so high as to constitute a significant part of the total

flaring over a year, a part which can be expected to have a significantly different molar mass from that the low flaring periods. This means that it will be almost impossible to obtain a representative CO_2 emission factor from gas samples, which typically will be taken during low flaring conditions.

Using an on-line gas chromatograph can possibly improve this, as a new sample is taken typically every 15 minute. However, gas composition during flaring events with a shorter time period than this, may not be measured. In addition, the flare gas is more complex than sales gas e.g. also in the sense that liquid may be present. This complicates the operation of the gas chromatographs, and thus this may not be a technically recommended solution.

In installations where the flaring is not more or less constant, there is therefore a need for new methods for cost-effective and precise estimation of the CO_2 emission factor. In the next section, such a method is proposed, based on the measurements carried out by the ultrasonic flare gas meter in addition to installation specific information.

Related to this discussion it should also be mentioned that there is a trend in the industry to change the reporting regime for fuel and flare gas from standard volume to mass. This is because the CO_2 emission factor has a much smaller change with change in gas composition when it is reported in kg/kg compared to when it is reported in kg/Sm^3. Thus, uncertainty limits are typically easier to meet for the CO_2 emission factor when it is reported in kg/kg. This is indicated in Figure 1, where the CO_2 emission factor in kg/kg and in kg/Sm^3 is plotted as a function of molar mass. The gas in this calculation consists of alkanes and a molar fraction of up to 1 % of nitrogen, carbon dioxide and water vapour respectively.

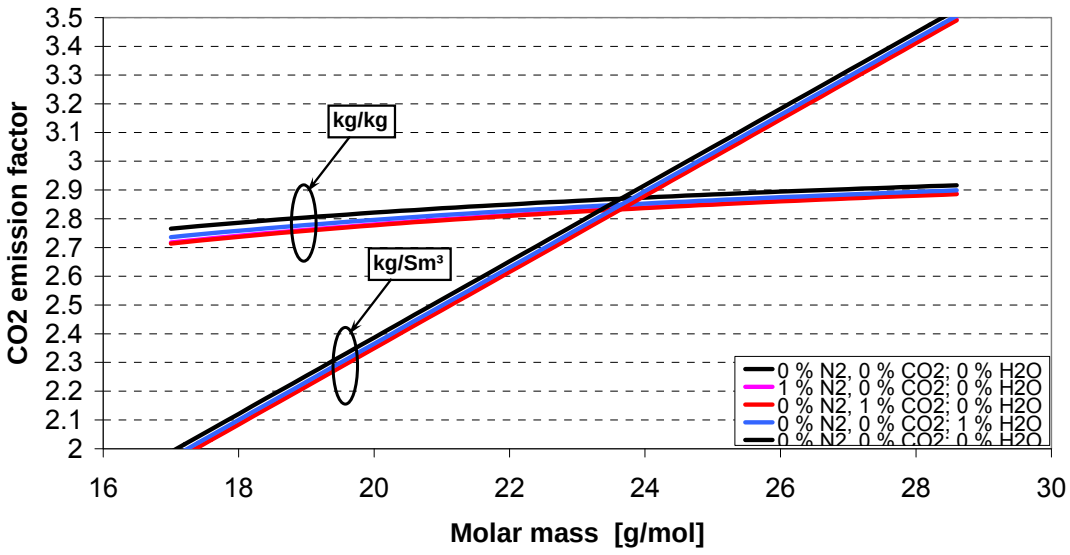

Figure 1: CO_2 emission factor as a function of molar mass, for pure alkanes, and alkanes with addition to a molar fraction of 1 % of nitrogen, carbon dioxide and water vapour, respectively.

4 NEW CO_2 EMISSION FACTOR ALGORITHM

In this chapter, the new method for estimation of the CO_2 emission factor in a cost-effective way for flaring systems is presented. The basic formulas are first derived. Thereafter there is a discussion on estimation of the inert gas content (N_2, CO_2, and H_2O) and uncertainties of such estimation.

4.1 Basic Formula

In general, the CO_2 emissions factor can be calculated from the molar fractions of each component in the flare gas, in the following way:

$$C_{C,M} = \frac{m_{CO2}}{m} \sum_{i=1}^{N} \phi_i n_i \quad (1)$$

$$C_{C,V} = C_{C,M} \rho_0 \quad (2)$$

where

$C_{C,M}$:	CO_2 emission factor, mass CO_2 per mass burnt gas
$C_{C,V}$:	CO_2 emission factor, mass CO_2 per volume (at standard pressure and temperature) burnt gas
ρ_0 :	gas density at standard pressure and temperature
m_{CO2} :	molar mass of CO_2.
m :	molar mass of the burnt gas.
ϕ_i :	molar fraction of gas component number *i* in the burnt gas.
n_i :	number of carbon atoms in the molecule of gas component number *i* in the burnt gas.
N :	total number of gas components in the burnt gas.

It has previously been considered to use knowledge about the plant, process simulation models and composition analysis of spot samples to estimate a likely average flaring composition and by that get an estimate of a fixed CO_2 emission factor. The uncertainty of such an approach would be high: A typical installation has many different sources to the flare system, with widely different compositions and thus widely different CO_2 emission factors. Since the relative contribution of each source varies over time, perhaps as much as 0 to 100%, the combined CO_2 emission factor for a flare varies widely. There is usually no metering of the individual sources and it is therefore not possible to keep track of the individual contributions to flaring. An improved method is needed, and a method has been found that utilizes the available data from the ultrasound meter. The data enables calculating the molar mass for a given period, as accumulated mass divided by accumulated moles, from which the average CO_2 emission factor for that period can be calculated.

Assuming a flare gas consisting of alkanes only, with molecular formulas CH_4, C_2H_6, C_3H_8, ..., the calculation of the CO_2 emission factor from the molar mass is exact. The general alkane formula is $C_nH_{(2n+2)}$, which is also valid for a mixture of alkanes, where *n* then becomes the average number of carbon atoms per molecule. Actually, the formula is also valid for a mixture of alkanes and hydrogen, as hydrogen (H_2) can be represented by $n = 0$ in $C_nH_{(2n+2)}$. Substituting C and H with molar masses of carbon and hydrogen (in form of single atoms and not in molecules) we get the following equation relating the molar mass, *m*, to *n* and the molar masses of carbon and hydrogen:

$$m = m_C n + m_H (2n+2) = 12.011n + 1.008(2n+2) \quad (3)$$

We are interested in finding *n*, from which the CO_2 emission factor can be calculated, and therefore we rearrange:

$$n = \frac{m - 2m_H}{m_C + 2m_H} = \frac{m - 2.016}{14.027} \quad (4)$$

We do not see pure alkane/hydrogen flare gas in practice and we therefore have to correct for the other components present, which can be unsaturated hydrocarbons as well as non-hydrocarbon inert gas components. For an offshore facility with separation of hydrocarbons, the amount of non-alkane hydrocarbons going to flare is small and thus the error from assuming that all hydrocarbons are alkanes or hydrogen is small. We do not normally see alkenes and alkynes with $n < 6$, and thus the unsaturated hydrocarbons tend to be heavy and stay in the liquid. For those that do evaporate, Eq. (4) would not give a very large error due to the dominance by mass of carbon. For example cyclo-hexane with $n = 6$, would get $n = 5.86$ by Eq. (4), while benzene would get $n = 5.43$.

The inert gas components, i.e. components that are neither hydrocarbon nor hydrogen, present in the flare gas must be corrected for. The experience from Statoil's offshore platforms is that only three inerts are present in significant amounts: Nitrogen, carbon dioxide and water. The content of these must be estimated separately by using knowledge about the plant, etc., as one would do for the hydrocarbons as well if the molar mass was not available. This means that by utilising the molar mass in the calculation of the CO_2 emission factor, one does not eliminate the uncertainty of composition estimation, but limits it to the inerts.

Eqs. (5) - (10) correct for inert mole fractions ϕ_{N2} ϕ_{CO2} and ϕ_{H2O}:

$$n = \phi_{HC} \frac{m_{HC} - 2m_H}{m_C + 2m_H} + \phi_{CO_2} \tag{5}$$

$$n = \frac{\phi_{HC} m_{HC} - 2m_H \phi_{HC}}{m_C + 2m_H} + \phi_{CO_2} \tag{6}$$

$$n = \frac{\phi_{HC} m_{HC} - 2m_H (1 - \phi_{N_2} - \phi_{CO_2} - \phi_{H_2O})}{m_C + 2m_H} + \phi_{CO_2} \tag{7}$$

The product of hydrocarbon mole fraction and molar mass, $\phi_{HC} m_{HC}$, in Eq. (7) is replaced with known values as shown in Eqs. (8) - (10).

$$m = \phi_{HC} m_{HC} + \phi_{N_2} m_{N_2} + \phi_{CO_2} m_{CO_2} + \phi_{H_2O} m_{H_2O} \tag{8}$$

$$\phi_{HC} m_{HC} = m - \phi_{N_2} m_{N_2} - \phi_{CO_2} m_{CO_2} - \phi_{H_2O} m_{H_2O} \tag{9}$$

$$n = \frac{m - \phi_{N_2} m_{N_2} - \phi_{CO_2} m_{CO_2} - \phi_{H_2O} m_{H_2O} - 2m_H (1 - \phi_{N_2} - \phi_{CO_2} - \phi_{H_2O})}{m_C + 2m_H} + \phi_{CO_2} \tag{10}$$

A CO_2 emission factor in kg CO_2 / Sm^3 gas can then be calculated from n using the molar mass of CO_2 and the molar volume of the gas at standard conditions:

$$C_{C,V} = \frac{m_{CO_2}}{V_{mol}} n \tag{11}$$

Similarly, a CO_2 emission factor in kg CO_2/kg gas can be calculated by Eq. (10):

$$C_{C,M} = \frac{m_{CO_2}}{m} n \tag{12}$$

In order to summarize, the CO_2 emission factor can be written in the following way under the assumption that the gas contains only hydrogen, alkanes, nitrogen, carbon dioxide and water vapour:

$$C_{C,M} = \frac{m_{CO2}}{m}\left(\frac{m-\phi_{N2}m_{N2}-\phi_{CO2}m_{CO2}-\phi_{H2O}m_{H2O}-2m_H\left(1-\phi_{N2}-\phi_{CO2}-\phi_{H2O}\right)}{m_C+2m_H}+\phi_{CO2}\right) \quad (13)$$

$$C_{C,V} = \frac{m_{CO2}}{V_{mol}}\left(\frac{m-\phi_{N2}m_{N2}-\phi_{CO2}m_{CO2}-\phi_{H2O}m_{H2O}-2m_H\left(1-\phi_{N2}-\phi_{CO2}-\phi_{H2O}\right)}{m_C+2m_H}+\phi_{CO2}\right) \quad (14)$$

where

m_{N2}:	molar mass of nitrogen, N_2
m_{CO2}:	molar mass of carbon dioxide, CO_2
m_{H2O}:	molar mass of water vapour, H_2O
m_H:	molar mass of hydrogen (just one atom), H
ϕ_{N2}:	molar fraction of nitrogen, N_2
ϕ_{CO2}:	molar fraction of carbon dioxide, CO_2
ϕ_{H2O}:	molar fraction of water vapour, H_2O
V_{mol}:	the molar volume

This means that the CO_2 emission factor can be found if the following input is known:

- molar mass of the flare gas
- molar fraction of nitrogen
- molar fraction of carbon dioxide
- molar fraction of water vapour

The ultrasonic flare gas meter is in principle a volumetric flow meter. Thus it accumulates standard volume of flare gas. In addition, the mass of flare gas can also be accumulated due to flare gas density estimates (from the velocity of sound). In the present algorithm, the accumulated standard volume and mass is used for calculation of an average flare gas molar mass.

The determination of the inert gas molar fractions (nitrogen, carbon dioxide and water vapour) will be addressed below.

4.2 Sources of Flare Gas

In order to address the determination of the molar fractions of the inert gas components (nitrogen, carbon dioxide and water vapour), installation specific information needs to be considered.

The flare gas in a specific installation may origin from several places in the process, including e.g.:

- Export gas
- First stage separator
- Second stage separator
- Compressor
- etc

The gas composition can be quite different for the gas from the various flare gas sources. If, for each of these flare gas sources, the molar mass and the molar fraction of nitrogen, carbon dioxide and water vapour is known either precisely or approximately.

In many cases the inert content will have some dependence on the molar mass of the flare gas. The model therefore requires that two sets of inert mole fractions are specified; one for a low molar mass and one for a high molar mass. Linear interpolation between the two is then used to find the set of inert mole fractions to be used together with the molar mass given by the ultrasound meter:

$$\phi_{N2} = \frac{m - m_{light}}{m_{heavy} - m_{light}} \phi_{heavy,N2} + \left[1 - \frac{m - m_{light}}{m_{heavy} - m_{light}}\right] \phi_{light,N2}$$

$$\phi_{CO2} = \frac{m - m_{light}}{m_{heavy} - m_{light}} \phi_{heavy,CO2} + \left[1 - \frac{m - m_{light}}{m_{heavy} - m_{light}}\right] \phi_{light,CO2} \quad (15)$$

$$\phi_{H2O} = \frac{m - m_{light}}{m_{heavy} - m_{light}} \phi_{heavy,H2O} + \left[1 - \frac{m - m_{light}}{m_{heavy} - m_{light}}\right] \phi_{light,H2O}$$

The nitrogen content tends to be high in low-molar mass gas, and low in high molar mass gas. The reason is that in a separation train most of the N_2 will go with the gas in the first stage separator. The gas from the first stage separator will have a high methane fraction and therefore a low molar mass, while gas from further separation stages will have heavier hydrocarbons and therefore a higher molar mass, and at the same time a lower N_2 fraction.

The water fraction will follow an opposite trend, as water vapour pressure divided by total pressure will be larger in the gas from the third stage separator than in the gas from the first. CO_2 does not have such clear-cut trend so it is mainly N_2 and H_2O that justify specifying two sets of inert mole fractions.

There may be cases where there is one or more sources to flare with a very high non-hydrocarbon content. If the amounts and compositions of these can be well estimated, one may be able to reduce the uncertainty by subtracting the inert part of these from the activity data before entering into the model.

Purge gas consisting mainly of nitrogen is usually metered separately, and can therefore easily be subtracted from the activity data.

Produced water degassing may also be a candidate for subtraction from the activity data, as long as only the inert part of it is subtracted. It does not follow the trend of increasing water vapour content with increasing molar mass valid for flare gas from the separation train, and linear interpolation between the two reference inert fraction sets based on flaring from the separation train will underestimate the water content. The methane part of the hydrocarbons bubbling out of the water is high, and the low total pressure combined with a fairly high temperature will give a large water vapour content even though the molar mass is low.

Subtraction of produced water degassing is less straightforward than for purge gas, because it is usually not metered directly, and because part of the water vapour can condense and drop out in the flare knock out drum.

In place of metering one can often assume the amount of gas from the water to be proportional to the amount of produced water, which is usually metered, and establish a factor, for example a gas water ratio GWR. The GWR depends on the amount of dissolved gas (determined by the conditions in the upstream vessels from which the water comes),

mostly light hydrocarbons, and the temperature, pressure and salinity, which dictate the water vapour fraction and how much of the dissolved gas is released. Process simulation software might be one way of estimating the GWR, but the common equations of state like SRK and PR with the classic mixing rules will not work, and a more advanced method is needed. For example, PVTsim with the Huron Vidal mixing rule can be used to estimate the GWR. The uncertainty must be expected to be significantly higher than one would expect for HC-HC flash calculations for which the common equations of state like SRK and PR are well suited. In addition to the rather high uncertainty of calculation, there is uncertainty due to varying pressure and temperature in the produced water degassing drum and in the vessels upstream feeding water to the degassing drum.

Before subtracting the inerts in the produced water degassing from the activity data, one should take into account condensation of water vapour in the knock out drum, which can be estimated using a process simulator. The amount of condensation in the knock out drum depends on the amount, temperature and water vapour content of other simultaneous sources, and is therefore uncertain.

As the above discussion shows, produced water degassing can introduce a large uncertainty. This uncertainty depends on how large a fraction of the total flaring the produced water degassing amounts to.

In case of a flare gas recovery system, the continuous produced water degassing will normally be recovered and returned to the process, and will only go to flare if there are upsets that send more gas to the flare than the recovery system has capacity for. In this case the produced water may constitute only a small fraction of the flaring and thus not give a large uncertainty.

If the plant has separate high and low-pressure flares, the produced water degassing will normally go the LP flare. If the produced water degassing makes up most or all of this flaring, it would be better not to subtract, and rather use its content of inerts as one of the two inert sets in the model.

If the sources to flare are normally so high in water vapour content that water will drop out in the knock-out drum, this must be taken into account when determining the sets of inert mole fractions to be entered into the model. The water vapour content is then given by the equilibrium water vapour pressure at the temperature measured at the ultrasound meter, which should be close to the temperature of the knock out drum. For large flare rates the pressure may be higher than atmospheric due to pressure drop in the stack, which should also be taken into account.

4.3 Summary of Algorithm

The proposed algorithm for calculation of the CO_2 emission factor can now be summarized in the following way:

- Measure gas volumetric flow rate and calculate molar mass in flare gas meter. The calculations depend on measured sound speed and measured temperature.
- Calculate standard volumetric flow rate by using measured pressure and temperature
- Calculate standard density from molar mass, standard pressure and standard temperature
- Calculate mass flow rate from standard density and standard volumetric flow rate
- Accumulate mass and standard volume
- Calculate average standard density from accumulated mass and accumulated volume
- Calculate average molar mass
- Calculate average mole fractions of N_2, CO_2 and H_2O from average molar mass and a heavy and light flare gas (both specified with molar mass and molar fractions of nitrogen, carbon dioxide and water vapour).
- Calculate average CO_2 emission factors, based on volume and/or mass.

5 UNCERTAINTY

5.1 Uncertainty Model

In the authority reporting of the climate gas emissions related to the burning of flare gas, also the uncertainty of the CO_2 emission factor needs to be addressed. In principle the CO_2 emission factor is calculated from the following four inputs:

- molar mass
- molar fraction of nitrogen
- molar fraction of carbon dioxide
- molar fraction of water vapour

The following uncertainty contributions will contribute to the overall uncertainty of the CO_2 emission factor estimate for the flare gas:

- Uncertainty in estimated molar mass from flare gas meter
  - Measured velocity of sound
  - Temperature measurement
  - Pressure measurement
  - Effect of accumulation
  - Model uncertainty
- Uncertainty in molar fractions N_2, CO_2 and H_2O
  - Effect from heavy and light gas simplification
  - Effect from uncertainty in molar mass
- Model uncertainty CO_2 emission factor
  - Non-ideal gases (Z-factor)
  - Non-alkanes

With the different terms as given above, the overall uncertainty model for the CO_2 emission factor can be written on relative form as

$$\left(\frac{u(C_C)}{C_C}\right)^2 = \left(\left(\frac{\partial C_C}{\partial m} + \frac{\partial C_C}{\partial \phi_{N2}}\frac{\partial \phi_{N2}}{\partial m} + \frac{\partial C_C}{\partial \phi_{CO2}}\frac{\partial \phi_{CO2}}{\partial m} + \frac{\partial C_C}{\partial \phi_{H2O}}\frac{\partial \phi_{H2O}}{\partial m}\right)\frac{m}{C_C}\frac{u(m)}{m}\right)^2 + \left(\frac{\partial C_C}{\partial \phi_{N2}}\frac{1}{C_C}u(\phi_{N2})\right)^2 + \left(\frac{\partial C_C}{\partial \phi_{CO2}}\frac{1}{C_C}u(\phi_{CO2})\right)^2 + \left(\frac{\partial C_C}{\partial \phi_{H2O}}\frac{1}{C_C}u(\phi_{H2O})\right)^2 + \left(\frac{u(C_{C,model})}{C_C}\right)^2 \quad (16)$$

Here, C_C means either $C_{C,V}$ or $C_{C,M}$, i.e. the volume based and the mass based CO_2 emission factor. It should be commented that the formula has been derived based on the functional relationship in Eqs. (14), (13) and Eq. (15). The uncertainty contributions to the estimated molar fractions of the three inert gas components are thus covered through the uncertainty of the molar mass, as this is the basic parameter for that estimation. The uncertainty contributions related to the assumption of the flare gas as a mixture of a light and a heavy flare gas is covered by the three terms addressing the uncertainty of each of these three molar fractions.

The partial derivatives can be found from Eqs. (13) , (14) and (15):

$$
\begin{aligned}
\frac{\partial C_{C,V}}{\partial m} &= \frac{m_{CO2}}{m}\left(\frac{1}{m_C + 2m_H}\right) \\
\frac{\partial C_{C,V}}{\partial \phi_{N2}} &= \frac{m_{CO2}}{V_{mol}}\left(\frac{-m_{N2} + 2m_H}{m_c + 2m_H}\right) \\
\frac{\partial C_{C,V}}{\partial \phi_{CO2}} &= \frac{m_{CO2}}{V_{mol}}\left(\frac{-m_{CO2} + 2m_H}{m_c + 2m_H} + 1\right) \\
\frac{\partial C_{C,V}}{\partial \phi_{H2O}} &= \frac{m_{CO2}}{V_{mol}}\left(\frac{-m_{H2O} + 2m_H}{m_c + 2m_H}\right) \\
\frac{\partial C_{C,M}}{\partial m} &= -\frac{C_{C,M}}{m} + \frac{m_{CO2}}{m}\left(\frac{1}{m_C + 2m_H}\right) \\
\frac{\partial C_{C,M}}{\partial \phi_{N2}} &= \frac{m_{CO2}}{m}\left(\frac{-m_{N2} + 2m_H}{m_c + 2m_H}\right) \\
\frac{\partial C_{C,M}}{\partial \phi_{CO2}} &= \frac{m_{CO2}}{m}\left(\frac{-m_{CO2} + 2m_H}{m_c + 2m_H} + 1\right) \\
\frac{\partial C_{C,M}}{\partial \phi_{H2O}} &= \frac{m_{CO2}}{m}\left(\frac{-m_{H2O} + 2m_H}{m_c + 2m_H}\right) \\
\frac{\partial \phi_{N2}}{\partial m} &= \frac{\phi_{heavy,N2} - \phi_{light,N2}}{m_{heavy} - m_{light}} \\
\frac{\partial \phi_{CO2}}{\partial m} &= \frac{\phi_{heavy,CO2} - \phi_{light,CO2}}{m_{heavy} - m_{light}} \\
\frac{\partial \phi_{H2O}}{\partial m} &= \frac{\phi_{heavy,H2O} - \phi_{light,H2O}}{m_{heavy} - m_{light}}
\end{aligned}
\tag{17}
$$

5.2 Uncertainty in Molar Mass

The first term on the right hand side of (3.2) gives the relative uncertainty contribution from the molar mass. The following uncertainty contributions are in principle identified with respect to the molar mass:

- Uncertainty in measured velocity of sound
- Uncertainty in temperature measurement
- Uncertainty if pressure measurement
- Uncertainty related to accumulation and assumption of light and heavy flare gas
- Uncertainty related to uncertainty in model for calculation of molar mass from velocity of sound

These uncertainty contributions are discussed below. It is found that the uncertainty contribution related to the uncertainty of the pressure measurement is negligible [2]. Thus, the following uncertainty model can be established for the molar mass:

$$\left(\frac{u(m)}{m}\right)^2 = \left(\frac{u(m_{VOS})}{m}\right)^2 + \left(\frac{u(m_T)}{m}\right)^2 + \left(\frac{u(m_{acc,\mathrm{mod}})}{m}\right)^2 \tag{18}$$

Uncertainty in measured velocity of sound: The molar mass of the flare gas is by the flare gas meter determined from the measured velocity of sound. Due to the low pressure, the flare gas is not far from an ideal gas. By applying the velocity of sound in an ideal gas, the following expression is found:

$$\left(\frac{u(m_{VOS})}{m}\right)^2 = \left(\frac{\partial m}{\partial c}\frac{c}{m}\frac{u(c)}{c}\right)^2 = \left(2\frac{u(c)}{c}\right)^2 \tag{19}$$

Uncertainty in temperature measurement: The uncertainty contribution of the molar mass due to uncertainty of the temperature measurement can be found from the ideal gas law as follows:

$$\left(\frac{u(m_T)}{m}\right)^2 = \left(\frac{\partial m}{\partial T}\frac{T}{m}\frac{u(T)}{T}\right)^2 = \left(\frac{u(T)}{T}\right)^2 \tag{20}$$

Uncertainty related to accumulation and assumption of light and heavy flare gas: In the application addressed in this paper, it is assumed that the flare gas consists of a heavy and a light flare gas contribution. The uncertainty component related to accumulation under this assumption this can be shown to be:

$$\begin{aligned}\frac{u(m_{acc})}{m} = &\left(\frac{m_{light}}{m}\right)\left(\frac{m_{heavy}-m}{m_{heavy}-m_{light}}\right)\left(\frac{u(m_{light,\mathrm{mod}})}{m_{light}}\right) \\ &+\left(\frac{m_{heavy}}{m}\right)\left(\frac{m-m_{light}}{m_{heavy}-m_{light}}\right)\left(\frac{u(m_{heavy,\mathrm{mod}})}{m_{heavy}}\right)\end{aligned} \tag{21}$$

It has been shown that other effects of accumulation are negligible, see [2].

Uncertainty related to uncertainty in model for calculation of molar mass from velocity of sound: The algorithm for calculation of the molar mass from the measured velocity of sound is meter specific. Due to confidential issues, the specific algorithms will not be given. Neither will the conclusions on the actual size of the uncertainty be given here. However, expressions to be used for Fluenta and GE ultrasonic flare gas meters have been given in [2]. It should be mentioned that it is possible to extend the method to also cover other vendors of ultrasonic flare gas meters.

5.3 Uncertainty in Molar Fractions of N_2, CO_2 and H_2O

The second line on the right hand side of (3.2) gives the relative uncertainty contribution from the molar fractions of N_2, CO_2 and H_2O. The following uncertainty contributions are in principle identified with respect to these molar fractions:

- Effect from uncertainty in molar mass
- Effect from heavy and light gas simplification

The first of these uncertainty contributions is covered in Section 5.2.

The effect from the heavy and light gas simplification is covered here.

The molar fractions of N_2, CO_2 and H_2O are determined by use of Eq. (15). The specified molar fractions of N_2, CO_2 and H_2O for the light and the heavy gas are thus interpolated. If there are other gas compositions that do not match this interpolation, an uncertainty contribution will occur. This is illustrated in Figure 2, where an example of a light gas with molar fraction of 22.79 g/mol and a nitrogen molar fraction of 0.9549 % is used together with a heavy gas with a molar fraction of 48.94 g/mol and a nitrogen molar fraction of 0.0331 %. The pink line then illustrates the molar fraction of nitrogen as a function of molar mass, as calculated by Eq. (15). The blue dots in the same plot indicate the gas quality that is expected to be flared from various parts of the process. The deviations between the pink line and the blue dots represents uncertainty due to molar fraction of the gas component in question (here nitrogen).

The uncertainty in the molar fraction of the inert gas components can be specified by the operator. However, a recommended value for the uncertainty is indicated based on up to 10 operator defined gas quality contributions to the flaring (the blue dots in Figure 2). The standard uncertainty in the molar fraction estimate is then recommended to be set to the standard deviation of the vertical difference between the blue dots and the pink line.

For CO_2 and H_2O the same procedure is followed as for nitrogen. It is assumed that H_2O is in its gaseous phase. If condensation is expected to take place in the flare drum, this must be corrected for.

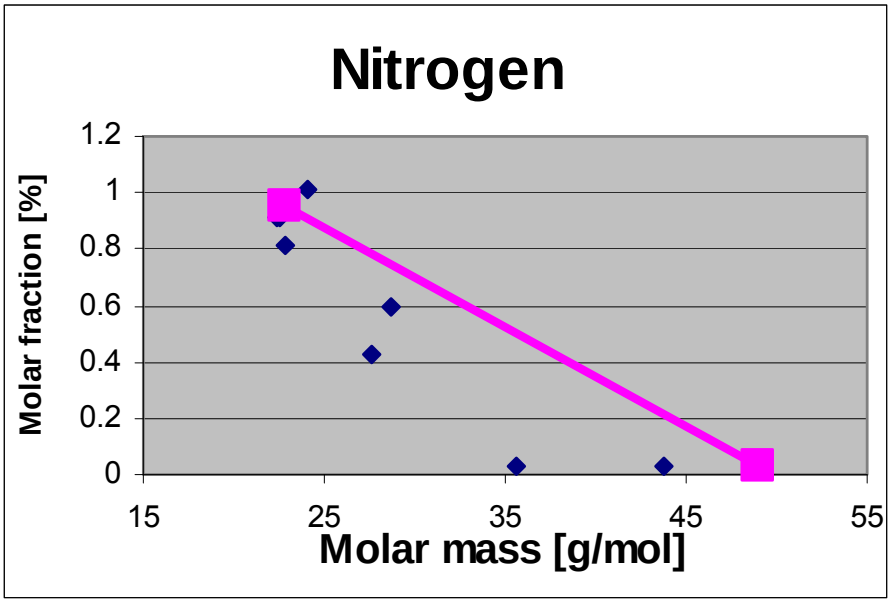

Figure 2: Interpolation of molar fraction of nitrogen, from a light and a heavy gas composition. Also included in the plot is molar fraction of nitrogen as a function of molar mass for 10 possible types of flare gas contributors. The example is synthetic, and generated with no specific installation in mind.

5.3 Model Uncertainty

The third line on the right hand side of (3.2) gives the relative uncertainty contribution from uncertainties in the model for calculation of the CO_2 emission factor from the molar mass and the molar fractions of N_2, CO_2 and H_2O itself (Eqs. (14) and (13)). Under the assumptions that the flare gas contains only alkanes, N_2, CO_2 and H_2O, this model is exact, except for compressibility effects (deviations from ideal gas). This effect is cancelled out in the mass based emission factor (Eq. (13)) while the relative uncertainty contribution will be the same as the relative uncertainty of the compressibility factor Z_0 at standard reference conditions, for the volumetric based CO_2 emission factor.

The compressibility factor at standard reference conditions can be shown to be mostly dependent on the molar mass for the gas components of relevance. It can be shown to be approximately equal to

$$\left(\frac{u(m_T)}{m}\right)^2 = \left(\frac{\partial m}{\partial T}\frac{T}{m}\frac{u(T)}{T}\right)^2 = \left(\frac{u(T)}{T}\right)^2 \tag{22}$$

$$Z_0 \approx 0.998 - \frac{(m-16)}{14}0.008 \tag{23}$$

By using Eq. (23), , the following expression is found for the relative standard uncertainty contribution due to model uncertainty:

$$\begin{aligned}\frac{u(C_{C,V,\text{model}})}{C_{C,V}} &= \frac{1}{\sqrt{3}}\left(0.002 + \frac{(m-16)}{14}0.008\right)\\ \frac{u(C_{C,M,\text{model}})}{C_{C,M}} &= 0\end{aligned} \tag{24}$$

This is based on the deviation from 1 for Z_0 that is taken as expanded uncertainty with rectangular probability distribution and 100 % confidence interval.

This is based on the deviation from 1 for Z_0 that is taken as expanded uncertainty with rectangular probability distribution and 100 % confidence interval.

5.4 Excel Spread Sheet

An Excel spread sheet has been developed to carry out the calculations of the CO_2 emission factor and the related uncertainty. The spread sheet has 6 sheets

- *README*
- *Gas input parameters*
- *Uncertainty*
- *Plot-uncertainty contribution*
- *Uncertainty guide*
- *Report CO_2*

In *README* a description of how to operate the spreadsheet is given; what is shown on the different sheets, which data input is necessary and where to seek assistance. The color code between input cells and calculated cells are also given.

In *Gas input parameter*s specifications like tags, years, flare gas meters and CO_2 emission factor (volume, mass) are given. Here also data for the light and heavy gas are given, and the measured accumulated flow data are given.

In *Uncertainty* the data for the uncertainties of measured temperature, measured speed of sound, H_2O; CO_2 and N_2 are given. A typical pressure and temperature value during flaring is also entered here[1].

The resulting uncertainty budget is shown in *Plot-uncertainty contribution*.

[1] These values are used in the estimation of the molar mass uncertainty.

In *Uncertainty guide* up to 10 different gases with input for molar mass and molar fractions of inert gases can be given. From the input suggested uncertainty in the inert gas molar fractions is calculated, this uncertainty is also shown in *Uncertainty* as a suggestion for the operator.

In *Report CO_2* the calculated CO_2 factor is shown and the resulting CO_2 emission for the gas rates given in *Gas input parameters*. The relative expanded uncertainty in the CO_2 factor is also given.

5.5 Calculation Example

Below, the actual Excel sheets are shown for a calculation carried out for a specific installation in Norwegian sector. The first data sheet, "Gas input parameters", is shown in Figure 3. Here, the type of flare gas meter, and the type of CO_2 emission factor (kg/kg or kg/Sm^3) is selected. Accumulated values of standard volume and mass of flare gas in 12 time periods (typically 12 months) can be specified. In addition, the light and heavy gas that the calculations assume the flare gas is a mixture of, is given.

A help for specification of the light and heavy gas can be found in the sheet "Uncertainty input guide". This is shown in Figure 4. Here, up to 10 different gases can be specified (molar mass and molar fraction of nitrogen, carbon dioxide and water vapour). These 10 gases are considered as being the typical sources of flare gas on the installation in question. In the plots at the bottom of that sheet, the molar fraction of nitrogen, carbon dioxide and water vapour, respectively, is plotted against the molar mass, for the 10 specified gases. In addition, the selected light and heavy gases, and the straight line between them, are shown. The closer to the straight line the dots representing the 10 gases are, the smaller is the uncertainty related to the estimation of the average molar fractions of nitrogen, carbon dioxide and water vapour. In addition, a recommended value for use as uncertainty related to the molar fraction of each of the three inert gas components is given.

In the sheet "Uncertainty budget", the recommended uncertainty values related to nitrogen, carbon dioxide and water vapour are found, see Figure 5. The user will have to specify the actual uncertainty values to be used related to the molar fraction of nitrogen, carbon dioxide and water vapour. This will often be the recommended value. In addition, uncertainty of the temperature measurement and the measurement of the velocity of sound must be given. In this example, expanded uncertainty with 95 % confidence level for the estimate of the temperature is taken as 0.3 °C, and for the estimate of the velocity of sound taken as 2 m/s. The basis for the uncertainty analysis in the temperature measurement is the specific routines and calculations carried out at the specific installation. For the uncertainty of the velocity of sound in a flare gas meter, not much information exists. However, based on [3], a value of 2 m/s has been selected as a typical but not low value. With this input, the sheet gives the uncertainty budget for the CO_2 emission factor. In this example, a relative expanded uncertainty with 95 % confidence level of 2.4 % is found.

In the sheet "Plot-uncertainty contributions" the various uncertainty contribution's impact on the output uncertainty (the relative expanded uncertainty of the CO_2 emission factor" is shown graphically, see Figure 6.

Finally, the sheet "Report CO_2" gives the CO_2 emission factor in addition to its relative expanded uncertainty with 95 % confidence level. Furthermore the total emission of CO_2 (mass) is given, see Figure 7.

Statoil

cmr Instrumentation

CO2 emission factor in flare systems, version 1.0

Gas input parameters

Specification of flaring system

Name of flaring system	**Platform Alpha, HP Flare**
Reporting period	**2009**
Type of flare gas meter	**Fluenta FGM 130/160**
Type of CO2 emission factor	**kg CO2/Sm³**

Specification of typical gas compositions

	Light gas		Heavy gas	
Molar mass	22.79	g/mole	48.94	g/mole
Molar fraction, N_2	0.9549	%	0.0331	%
Molar fraction, CO_2	0.5734	%	0.204	%
Molar fraction, H_2O	1.127	%	2.284	%

Measured flow data

Measured accumulated flare gas values	**MASS**		**VOLUME**	
Time period no. 1	417 029	kg	374 026	Sm³
Time period no. 2	1 412 388	kg	1 228 239	Sm³
Time period no. 3	604 866	kg	585 262	Sm³
Time period no. 4	304 209	kg	282 444	Sm³
Time period no. 5	524 113	kg	492 561	Sm³
Time period no. 6	748 956	kg	674 605	Sm³
Time period no. 7	1 031 172	kg	911 023	Sm³
Time period no. 8	618 694	kg	557 210	Sm³
Time period no. 9	557 122	kg	517 969	Sm³
Time period no. 10	551 857	kg	507 923	Sm³
Time period no. 11	570 280	kg	497 417	Sm³
Time period no. 12	1 099 384	kg	907 685	Sm³
Total	8 440 070	kg	7 536 365	Sm³

Figure 3: Gas input parameter sheet

Statoil

cmr Instrumentation

CO2 emission factor in flare systems, version 1.0

Uncertainty input guide

This worksheet is a guide for determination of the input uncertainty for the inert gas components, based on the gas composition of up to 10 sources for the flare gas

Flare gas source no.	Name of gas source	Molar mass		Molar fractions [%] N2		CO2		H2O		Operator comments:
1	Fuel gas	22.42	g/mol	0.912	%	0.708	%	0.0053	%	
2	Gas from LLP separator	48.94	g/mol	0.0331	%	0.204	%	2.283	%	Used as heavy in Gas input param.
3	Gas from LP separator	35.55	g/mol	0.0259	%	0.545	%	2.295	%	
4	Gas from MP separator	27.65	g/mol	0.427	%	0.6995	%	1.5105	%	
5	Gas from LP inlet separator	22.82	g/mol	0.8167	%	0.6907	%	1.762	%	
6	Gas from HP inlet separator	22.79	g/mol	0.9549	%	0.5734	%	1.127	%	Used as light in Gas input param.
7	Alternative flaring case LP inlet sep.	28.62	g/mol	0.595	%	0.594	%	1.899	%	
8	Alternative flaring case LP + LLP	43.83	g/mol	0.03	%	0.334	%	2.287	%	
9	Export gas case A	24.02	g/mol	1.0157	%	0.627	%	0.0053	%	
10	Export gas case B	22.47	g/mol	0.911	%	0.7077	%	0.0053	%	
Suggested uncertainty (95 % c. l.)				0.42	%	0.23	%	1.41	%	

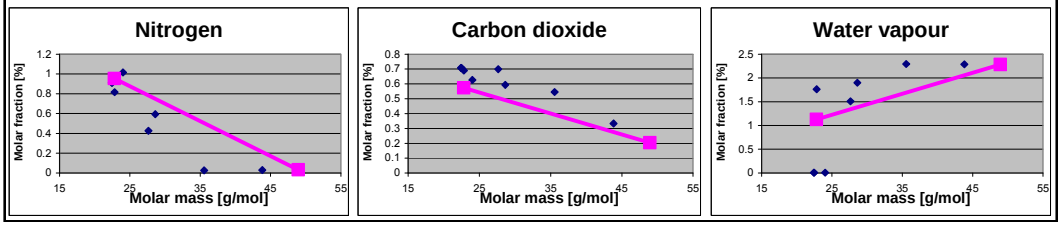

Figure 4: Uncertainty input guide sheet

Statoil

cmr Instrumentation

CO2 emission factor in flare systems, version 1.0

Uncertainty budget

Typical pressure	1	bara
Typical temperature	20	°C

Input variable	Given Uncertainty		Confidence Level (probability distr.)	Type of uncertainty	Standard Uncertainty		Sensitivity Coefficient	Variance	
Temperature measurement	0.3	°C	95 % (normal)	B	0.15	°C	0.0120593	3.272E-06	(kg CO2/Sm³)²
Velocity of Sound measurement	2	m/s	95 % (normal)	B	1	m/s	0.0204401	0.0004178	(kg CO2/Sm³)²
Model uncertainty molar mass	1.241	%	95 % (normal)	B	0.621	%	0.0353519	0.0004814	(kg CO2/Sm³)²
Nitrogen	0.42	%	95 % (normal)	B	0.21	%	0.0344959	5.248E-05	(kg CO2/Sm³)²
(recommended value nitrogen	0.42	%	)						
Carbon dioxide	0.23	%	95 % (normal)	B	0.115	%	0.0371095	1.821E-05	(kg CO2/Sm³)²
(recommended value carbon dioxide	0.23	%	)						
Water vapour	1.41	%	95 % (normal)	B	0.705	%	0.0212295	0.000224	(kg CO2/Sm³)²
(recommended value water vapour	1.41	%	)						
Emission factor model	0.799	%	100 % (rectangular)	B	0.4612314	%	0.0317103	0.0002139	(kg CO2/Sm³)²

CO2 emission factor estimate			
	Sum of variances, $u_c(C)^2$	0.0014111	(kg CO2/Sm³)²
	Combined Standard Uncertainty, $u_c(C)$	0.0376	kg CO2/Sm³
	Expanded Uncertainty (95% confidence level, k=2), k $u_c(C)$	0.0751	kg CO2/Sm³
	Value of CO2 emission factor	3.1710294	kg CO2/Sm³
	Relative Expanded Uncertainty (95% confidence level, k=2), k EC	2.3692	%

Figure 5: Uncertainty budget sheet

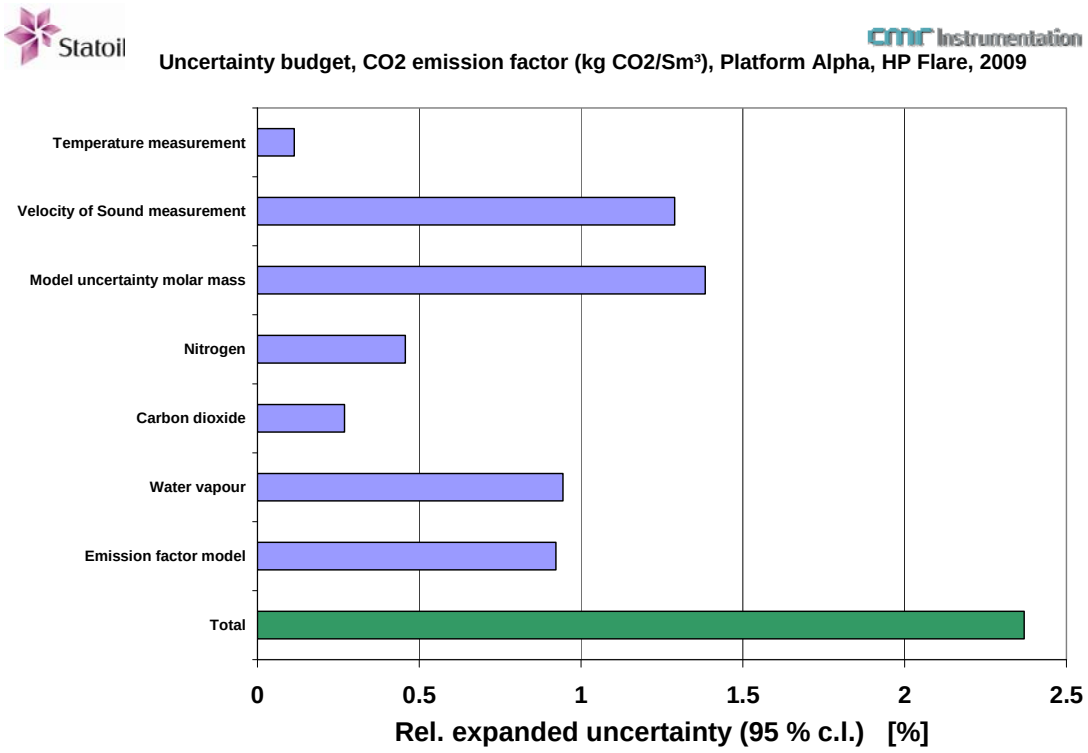

Figure 6: Plot-uncertainty contributions sheet

Statoil

cmr Instrumentation

CO2 emission factor in flare systems, version 1.0

CO2 - report

Name of flaring system	Platform Alpha, HP Flare	
Reporting period	2009	

	CO2 EMISSION FACTOR		CO2 EMISSION	
Time period no. 1	3.155	kg CO2/Sm³	1180	ton CO2
Time period no. 2	3.266	kg CO2/Sm³	4011	ton CO2
Time period no. 3	2.898	kg CO2/Sm³	1696	ton CO2
Time period no. 4	3.036	kg CO2/Sm³	857	ton CO2
Time period no. 5	2.995	kg CO2/Sm³	1475	ton CO2
Time period no. 6	3.140	kg CO2/Sm³	2119	ton CO2
Time period no. 7	3.209	kg CO2/Sm³	2923	ton CO2
Time period no. 8	3.141	kg CO2/Sm³	1750	ton CO2
Time period no. 9	3.031	kg CO2/Sm³	1570	ton CO2
Time period no. 10	3.066	kg CO2/Sm³	1557	ton CO2
Time period no. 11	3.255	kg CO2/Sm³	1619	ton CO2
Time period no. 12	3.459	kg CO2/Sm³	3140	ton CO2
Total	3.171	**kg CO2/Sm³**	23898	**ton CO2**
Rel. exp. uncertainty (95 % conf. level)	2.4	%		

Figure 7: CO_2 - report sheet

6 INDUSTRIAL EXPERIENCE WITH THE NEW MODEL

Per 2009 Statoil operates totally 31 offshore production facilities; and typical 1 – 3 flare gas metering systems in use on each facility.

Experience highlights:

- During first reporting period, 2009, the method have been in use for calculation of specific emission factor at 16 of 31 offshore production facilities
- By proper documentation of input data; the model have been accepted by the Norwegain Pollution Agency (KLIF / formerly SFT)
- Installations and facilities where the new method have been implemented, have experienced approximately 25% lower annual CO_2 reported quantities from flare gas systems compared to the default emission factor.
- The new method is considered as an improvement which better reflect the actual flared CO_2 quantities.
- Close cooperation between metering and process discipline is a criteria for successful implementation and use of the model
- Logging of interdependent accumulated figures (mass and standard volume) requires a logging system to be in place; some installation have required upgrade in control system
- Generation and definition of gas molar mass and inert gas content have been complex
- Model has currently no functionality for deduction of purge gas (N_2). This is possible to implement in future.
- Model not fully suitable for flare gas systems exposed with a huge span of the inert gas content; typically where produced water degassing constitutes a large fraction of the flare gas and for CO_2 removal facilities like e.g. Sleipner T.

7 CONCLUSIONS AND SUMMARY

In the present paper, a new and cost-effective method for calculation of the CO_2 emission factor for flaring systems is presented. The development of the method is motivated by the new authority requirements related to CO_2 emissions. Discussions related to these requirements have touched solutions like daily gas sampling and laboratory analyses, or online gas chromatography on the flare line. Such solutions may be technologically challenging, and are also expensive with respect to costs and man hours.

The cost-effective alternative that is presented here is based on measurements that are already performed, by ultrasonic flare gas meters. In addition, installation specific gas quality information is needed, on a general level.

An uncertainty model has also been developed for the method. An Excel program has been developed for calculation of the CO_2 emission factor, and for the uncertainty analysis. The actual uncertainty that is obtained depends on the installation, and especially on the gas composition of each of the sources of gas (like export gas, compressor gas, gas from separator, etc.) to the flare.

The new method has been taken into use on several of Statoil's installations.

8 REFERENCES

[1] Guidelines for the monitoring and reporting of greenhouse gas emissions pursuant to Directive 2003/87/EC of the European Parliament and of the Council, 2006.

[2] Hallanger, A., Frøysa, K.-E. and Bjørk, R. N.: "CO_2 emission factor for flaring systems – methodology and uncertainty estimate," CMR report no. CMR-09-F10063-RA-1-Rev01, Christian Michelsen Research AS, Bergen, Norway, 2009 (Confidential).

[3] Frøysa, K.-E., Ekerhovd, H. and Johannessen, A. A.: "Nitrogen subtraction on reported CO_2 emission using ultrasonic flare gas meter," 27th North Sea Flow Measurement Workshop, Tønsberg, Norway, October 2009.